PARTICLE AND GASEOUS EMISSIONS FROM MODERN MASONRY HEATER

Konsta Kulmala
Particle and gaseous emissions from modern masonry heater
Master of Science thesis
Environmental Science Major
University of Eastern Finland, Department of Environmental Science
January 2014

ABSTRACT

The aim of this thesis was to investigate particle and gaseous emissions from modern masonry heater during the batch combustion of wood. Different continuous devices and filter collection methods were applied in the experiments. The applicability of a novel sampling method for measuring particle mass concentration was tested. The obtained results were compared to each other and to the proposed limit values in the upcoming legislation of the European Union.

In Finland wood combustion has long traditions and it is still popular. In fact, during the last ten years the popularity of it has even increased. Wood fuel is easy to access and it is cheap compared to other heat sources. One possible contribution to the increased wood combustion has been the new energy policy of the EU which supports the use of renewable energy.

Measuring the particle emissions from residential wood combustion (RWC) is important because of the health effects of the particles. In addition, atmospheric particles affect the Earth's radiation balance. RWC is a significant source of particle emissions. Unlike in power plants, in RWC appliances the flue gases are rarely purified and emissions are usually easily transported to the human breathing zone. EU is about to set emission limits for the RWC appliances. In EU a common method for measuring the emissions from small-scale biomass combustion is still missing and this is why it is important to develop and test different methods.

Majority of the emissions were formed during the first batch. Fine particles (particles below 2.5 μm in aerodynamic diameter) dominated the particle mass emissions. The share of light absorbing carbon (BC, i.e. soot) in the fine particles was very high when compared to other previously studied small-scale appliances. The main reason to this was most likely too small furnace. The flame temperature probably decreased when it was in contact to the window and to the walls of the furnace which led to incomplete combustion of the soot particles.

The gaseous emissions from the studied masonry heater were very low. All of the gaseous emissions which will be regulated in the future (carbon monoxide, organic carbon, oxides of nitrogen) were below the limit values. Fulfilling the particle emission limit depended on the applied method. Particle mass concentration in the hot and undiluted flue gas fulfilled the requirements but the concentration in the diluted sample was about 1.5-fold to the emission limit.

Keeping the dilution stable in the novel sampling method required plenty of monitoring and adjusting. The filter collection itself was fluent to execute. To make the system more transportable the structure of it could be reconsidered.

TIIVISTELMÄ

Tutkielman tavoitteena oli selvittää modernin varaavan takan hiukkas- ja kaasupäästöt puun panospolton aikana. Työssä käytettiin erilaisia jatkuvatoimisia mittalaitteita ja kerääviä näytteenottomenetelmiä. Lisäksi testattiin uuden näytteenottomenetelmän soveltuvuutta hiukkasmassapitoisuuden määrittämiseen. Eri mittaustekniikoiden tuloksia verrattiin toisiinsa sekä tuleviin Euroopan unionin lainsäädännössä ehdotettuihin raja-arvoihin.

Pienpoltolla on Suomessa pitkät perinteet ja puuta poltetaan yhä paljon, viimeisen kymmenen vuoden aikana jopa lisääntyvissä määrin. Syitä tähän ovat polttopuun helppo saatavuus ja edullisuus suhteessa muihin lämmönlähteisiin. Euroopan unionin uusiutuvaa energiaa suosivan energiapolitiikan myötä puun pienpolton ei ainakaan odoteta vähenevän.

Pienpolton hiukkasia mitataan niiden terveysvaikutusten takia. Lisäksi hiukkaset vaikuttavat erilaisin tavoin maapallon säteilytasapainoon. Puun pienpoltto on merkittävä hiukkasten päästölähde. Toisin kuin suurissa polttolaitoksissa, pienpolton päästöjä ei juurikaan hallita puhdistimilla ja ne kulkeutuvat usein nopeasti ihmisten hengitysvyöhykkeelle. EU:ssa ollaan asettamassa uusille pienpolttolaitteille päästörajoituksia. Yhtenäistä EU:n laajuista mittausmenetelmää biomassan pienpolton hiukkaspäästöille ei kuitenkaan ole vielä olemassa, ja siksi eri menetelmien kehittäminen ja testaus on tärkeää.

Valtaosa puun panospolton päästöistä muodostui ensimmäisen panoksen aikana. Valtaosa muodostuneiden hiukkasten massasta koostui pienhiukkasista (aerodynaamiselta halkaisijaltaan alle 2.5 μm hiukkaset). Työssä tutkittu takka poikkesi muista aikaisemmin tutkituista pienpolttolaitteista siten, että valtaosa pienhiukkasista koostui valoa absorboivasta mustasta hiilestä, eli noesta. Suurin syy tähän oli todennäköisesti pieni tulipesä. Liekin lämpötila luultavasti aleni sen ollessa kosketuksissa tulipesän luukun lasiin sekä seinämiin, minkä seurauksena nokihiukkaset paloivat epätäydellisesti.

Takasta mitatut kaasumaiset päästöt olivat erittäin alhaiset. Tulevat päästövaatimukset täyttyivätkin kaikkien säädeltyjen kaasumaisten päästöjen (häkä, orgaaninen hiili, typen oksidit) osalta, mutta hiukkaspäästörajan täyttyminen riippui käytetystä menetelmästä. Mitattaessa kuumasta laimentamattomasta savukaasusta hiukkasmassapitoisuus oli alle päästörajan, laimennetun näytteen pitoisuus ylitti päästörajan noin 1.5-kertaisesti.

Testattu uusi hiukkasmittausmenetelmä vaati paljon monitorointia ja säätöä savukaasun laimennuksen osalta. Suodatinkeräyksen toteuttaminen oli sujuvaa. Mikäli laitteistoa on tarkoitus siirtää mittauspaikalta toiselle, sen liikuteltavuutta on syytä parantaa.

ACKNOWLEDGEMENTS

ABBREVIATIONS AND SYMBOLS

BC	Black carbon
d_p	Particle diameter
CMH	Conventional masonry heater
DR	Dilution ratio
EC	Elemental carbon
ED	Ejector diluter
FID	Flame ionization detector
FTIR	Fourier transform infrared spectroscopy
GMD	Geometric mean diameter
HC	Hydrocarbon
MMH	Modern masonry heater
OC	Organic carbon
OGC	Organic gaseous compounds as measured with FID
PAH	Polycyclic aromatic hydrocarbon
PB	Pellet boiler
PM	Particulate matter
PM_x	Mass of particles below aerodynamic diameter of x µm
POM	Particulate organic matter
PRD	Porous tube diluter
RWC	Residential wood combustion
SOA	Secondary organic aerosol
SS	Sauna stove
TS-MMH	This study-modern masonry heater
TSP	Total suspended particles
VOC	Volatile organic compound
WS	Wood stove
λ, lambda	Air-to-fuel ratio, the ratio between actual oxygen demand and stoichiometric oxygen demand

Contents

APPENDICES

1. INTRODUCTION

The sources of fossil fuels (e.g. oil, coal, natural gas) are limited and strengthening of the greenhouse effect is a well-recognized fact among the scientific community. Therefore, European Union has given a renewable energy -directive (2009/28/EC) to increase the use of renewable energy sources in the energy production and to diminish greenhouse gas emissions. According to the directive 20 % of the total European Union energy demand has to be met by renewable sources by the year 2020, for Finland the target is 38 %. This has increased the combustion of biomass, such as wood fuels. Globally, in the year 2005 utilizing biomass was estimated to cover over 10 % of the annual primary energy use ($\approx$ 470 EJ), utilizing fossil fuels around 80 %. The remaining 10 % was attributed to nuclear power and renewables other than biomass (Sims et al., 2007).

Human exposure to increased concentrations of particulate matter (PM) in the respiratory air has been associated to damaging health effects such as cardiopulmonary and respiratory illnesses (Pope & Dockery, 2006; WHO, 2006). Epidemiological evidence shows that adverse health effects occur due to both short-term and long-term PM-exposure. A threshold, below which no health effects occur, cannot yet be determined or the evidence of it is weak. (WHO, 2006). Statistically, in the European Union region, exposure to PM caused almost 350,000 premature deaths and resulted in direct and indirect economic consequences equivalent to approximately 270 billion euros in the year 2000 (European Commission, 2005). In addition, PM affects the Earth's radiation balance by scattering (primarily sulphate, nitrate, mineral dust) and absorbing (black carbon, BC) the straight radiation coming from the Sun. BC weakens the Earth's surface albedo when it deposits on snow and ice. The most complicated climate effect of particles is that they modify the optical properties and the lifetime of clouds. According to the current state of scientific knowledge the net effect of PM on climate is estimated to be cooling but all the effect mechanisms are not yet clearly understood. (Forster et al., 2007.)

Residential wood combustion (RWC) is a great contribution to the levels of fine particle ($PM_{2.5}$, particle mass below aerodynamic size of 2.5 µm) and gaseous emissions in the outdoor air (Szidat et al., 2007; Hellén et al., 2008). Glasius et al. (2006) noticed that $PM_{2.5}$ levels measured in a residential heating area were comparable to the levels measured at a busy street with plenty of traffic. The main source of $PM_{2.5}$ in Finland is long-range transport which

is estimated to account for 64-76 % of the $PM_{2.5}$ concentration in Helsinki urban air (Karppinen et al., 2004). However, of the national primary $PM_{2.5}$ emissions RWC accounted for 25 % in the year 2000 (Karvosenoja et al., 2008). What makes RWC so special is that the combustion takes place in the centers of population and stack heights are low. Consequently, the emissions are easily transported to the human breathing zone. Variety of different combustion appliances and fuels is large, appliances often lack the control of combustion conditions and flue gases are rarely purified. In addition, appliances are sometimes inappropriately operated. This is why emissions from RWC can be very versatile.

The energy efficiency -directive (2009/125/EC) is setting new requirements for energy-related products, also for RWC appliances. In relation to the directive the EuP Lot 15 -working group is contemplating emission standards for the appliances. In fact, some proposals have already been made (European Commission, 2013). Due to this manufacturers are more and more interested in developing their products for them to meet the upcoming standards.

In this thesis the particle and gaseous emissions from wood combustion in batch-wise operated masonry heater are measured. Measurements are executed in laboratory circumstances from a real RWC appliance used in Finland. The main attention in the literature review is in the formation of emissions and in the emission measurements.

2. LITERATURE REVIEW

2.1 RESIDENTIAL WOOD COMBUSTION

2.1.1 Relevance in residential energy production

The total energy consumption of residences in Finland in the year 2011 was approximately 62 gigawatt hours (GWh) of which heating of households covered 84 % (52 GWh) and household appliances 16 % (10 GWh). The most common source of residential heat was district heating (33 %), followed up by wood fuel (27 %) and electricity (23 %). (Statistics Finland, 2012.)

In RWC, batch combustion (e.g. masonry heaters, wood stoves, wood log boilers) and continuous combustion appliances (e.g. pellet burners and boilers, stoker burners) are in use (Tissari, 2008). The total amount of wood combusted in Finnish households and summer cottages in 2010 was estimated to be 8 million m^3. Popularity of RWC has grown 49 % (from 40 to 60 PJ a^{-1}) between the years 2000-2010. Of all the RWC-based energy in Finland 26 % was produced in boilers, 24 % in masonry heaters, 18 % in baking and other ovens, 15 % in sauna stoves, 11 % in other stoves and 6 % in fireplaces. (Karvosenoja et al., 2012.)

RWC is popular in Finland because it has long traditions and wood fuel is easy to access. The prices of some principal fossil fuels, excluding coal, have gone up which surely favors the use of wood fuel (Statistics Finland, 2013). Furthermore the European energy and climate policy supports RWC. Nowadays it is possible for Finnish citizens to get governmental funding if they want to invest in renewable energy or to improve the energy efficiency of the residence. In the year 2013 the amount of governmental funding for residential renovation alone was 2 million euros. (ARA, 2013).

2.1.2 Composition of wood fuel

In general, wood contains considerable amount of volatile species, 80-90 % by dry weight. Water content is high, typically 40-60 % by dry weight so the wood fuel must be dried before combustion to water content of approximately 15-20 %. The most common elements of wood are carbon (C), hydrogen (H) and oxygen (O) which altogether account for 99 % of wood's

dry weight. The shares of nitrogen (N) and sulphur (S) are less than 0.2 % and 0.05 %, respectively. The inorganic mineral content (i.e. ash) is less than 0.5 % which is low in contrast to other solid fuels, like peat (5 %) or charcoal (15 %). Typical minerals and trace elements are phosphorus (P), potassium (K), calcium (Ca), magnesium (Mg), manganese (Mn), iron (Fe), zinc (Zn), boron (B), copper (Cu) and chlorine (Cl). In spite of low ash content, volatile ash compounds (K, S, Cl, Zn) are important regarding emissions since they take part to the formation of fine fly ash (see section 2.2.4). (FINE, 2013; VTT, 2000.)

The structural composition of wood is cellulose (40-45 %), hemicellulose (25-40 %) and lignin (16-33 %). Lignin is essential for the structure since it bonds the fibers together and makes the overall structure strong. Lignin also contains plenty of carbon and hydrogen which produce a lot of heat during the combustion process. Less than 5 % of the structure consists of different extracts, like terpenes, fats and phenols. The shares of different components can differ between tree species and parts of the tree, for instance, between bark and stem wood. (VTT, 2000.)

2.1.3 Combustion process

In combustion fuel reacts with oxygen and heat energy is produced. The combustion reaction to be possible three conditions must be available: fuel, sufficient rate of heat and oxygen. The combustion of solid fuel is actually a combination of gasification of the fuel and oxidation of gaseous compounds. The process can be divided into energy consuming (drying and pyrolysis) and energy producing (combustion of pyrolysis products and char) stages. After the ignition the fuel particle heats up and water evaporates from the particle. Pyrolysis is the gasification of volatile compounds caused by the heat. As a result of pyrolysis the solid fuel particle is transformed into gaseous and tar-like substances. Next step is the homogeneous combustion of pyrolysis products. Final stage is the combustion of char which is the remains of fuel after pyrolysis. The char combustion is heterogeneous because reactions happen between gaseous oxygen and solid char. In practice the combustion stages overlap, i.e. combustion can take place at the surface while the core of the fuel particle is still drying. (FINE, 2013; Kilpinen, 2002a; Saastamoinen, 2002.)

In the combustion of solid fuels the transfer of reactants and air in and out the combustion reaction happen with diffusion. This means that the mixing of fuel and air occur in the flame.

Outside the flame is an air-rich, inside the flame a fuel-rich zone. Hence, combustion air diffuses in and fuel diffuses out which causes the mixing. This type of flame is called diffusion flame. When the fuel and air are mixed prior to combustion (e.g. in combustion engines) the flame is called premixed flame. (Flagan and Seinfeld, 1988.)

An ideal combustion produces only carbon dioxide (CO_2) and water vapour (H_2O). In real life, combustion is never ideal. This is the case especially with the batch combustion of wood. Particle and gaseous emissions are always formed. The most important conditions resulting in a good combustion are high combustion temperature, sufficient air supply and efficient mixing of combustion air and pyrolysis products. High temperature and sufficient air supply together make combustion reactions more complete and faster. However, these two are related to each other. To ensure adequate air supply in RWC, one is forced to feed more air than it is actually needed according to stoichiometry ($\lambda > 1$). This lowers the combustion temperature since warming up the inert N_2 in the air consumes plenty of heat energy. Modern RWC appliances are made to achieve high temperatures. For instance, the furnace is well isolated and the material reflects all the heat into the combustion process. The optimum mixing of flue gases and air is achieved with advanced air staging. Air is staged in two, sometimes in three sections. Primary air flows in under the grate which induces a powerful pyrolysis. Secondary and possibly tertiary airs are fed into the pyrolysis products and the combustion becomes more complete. The ratio between primary air and secondary air is crucial when it comes to emissions. If it is too high, pyrolysis is too strong and gases do not have time to go through combustion. The overall too low air supply can cause smouldering combustion with high emissions. Extremely high emissions form when the ratio of primary air and secondary air is wrong, batch size is big and log size is small. (FINE, 2013.)

2.2 FORMATION OF EMISSIONS

Flue gas contains gases, vapours and particulate matter. Together they form combustion aerosol. The main components of flue gas are gaseous N_2, O_2, CO_2 and vaporous H_2O. (Jokiniemi and Kauppinen, 2002; Tissari 2008.)

2.2.1 Carbon oxides

CO_2 is the strongest contributor to the climate change out of all the anthropogenic greenhouse gas emissions (Forster et al., 2007). Complete combustion of any carbon containing matter produces CO_2. The level of atmospheric CO_2 in September 2013 was 393.9 ppm molar (Cape Grim Greenhouse Gas Data, 2013).

Carbon monoxide (CO) is a product and a good indicator of incomplete combustion. It is formed mainly in the course of incomplete combustion during the ignition and heterogenic char combustion. CO being quite unstable molecule is eventually oxidized to CO_2 in a reaction with O_2 or with free radicals, like hydroxyl radical (OH^-), an important radical in the atmosphere. (FINE, 2013; Flagan and Seinfeld, 1988.)

2.2.2 Nitrogen oxides

Nitrogen oxides (NO_x) cause acidification, respiratory symptoms and they take part to photochemical reactions leading to forming of smog and tropospheric ozone (O_3) (Kilpinen, 2002b.) Jucks et al. (1996) state that in stratosphere, catalytic cycles of NO_x dominate the O_3-loss for altitudes between 24 and 38 km.

The sources of nitric oxide (NO) and nitrogen dioxide (NO_2), together referred as NO_x, are atmospheric N_2 or N-containing compounds in the fuel. In combustion a vast majority of NO_x is NO and the share of NO_2 is less than 5 %. Later in the atmosphere NO is effectively oxidized to NO_2. (Kilpinen, 2002b.)

Three main pathways leading to NO_x emissions can be distinguished. Thermal NO_x is formed when atmospheric N_2 breaks down and oxidizes in high temperatures (T > 1400 °C), so the role of it is negligible in RWC. The key to thermal NO_x formation are the reactions of N_2 with O- and OH-radicals. The formation of it speeds up drastically when 1600 °C is reached. Thermal NO_x formation is also known as Zeldovich mechanism. (Kilpinen, 2002b.)

A lot faster pathway is oxidation of N_2 with the catalytic help of fuel hydrocarbons (HC), especially hydrogen cyanide (HCN). Required temperatures are significantly lower than with

thermal NO_x. This process is called prompt NO, or the Fenimore mechanism. (Kilpinen, 2002b.)

In RWC almost all of the NO_x is originated from organic fuel-N which is highly reactive. The nitrogen in fuels is present predominantly in pyridine, pyrrole and amino groups. The formation is fast and not so dependent on temperature. RWC produces also minimal amounts of nitrous oxide (N_2O, laughing gas). A portion of N_2O is oxidized to NO_x. (Kilpinen, 2002b.)

2.2.3 Gaseous hydrocarbons and sulphur oxides

HC emissions originate from the volatile organic compounds (VOC) of the wood during pyrolysis. The number of different HCs is vast. They can be separated to aliphatic (C_xH_y) and aromatic compounds which contain a benzene ring (C_6H_6). The most common aliphatic HC is methane (CH_4) which is a strong greenhouse gas. Polycyclic aromatic hydrocarbons (PAHs) contain several benzene rings and are under a particular interest because some of them (like benzo[a]pyrene, $C_{20}H_{12}$) are proven to be carcinogenic. HCs are very reactive and can form new compounds with other elements, such as chlorine benzene (C_6H_5Cl) and furan (C_4H_4O), respectively. Other common HCs are aldehydes, ketones and different organic acids. (FINE, 2013; Huotari and Vesterinen, 2002.)

Like NO_x sulphur dioxide (SO_2) and sulphur trioxide (SO_3), together referred as SO_x, cause acidification and respiratory illnesses. Most of the primary emission is SO_2 and all of it originates from fuel-S. Because of the low sulphur content in wood the SO_x emissions from RWC are low compared to coal and oil. Natural gas is practically sulphur-free. In power plants SO_x is problematic because together with water it forms sulphuric acid (H_2SO_4) which causes damaging corrosion. (Iisa et al., 2002.)

2.2.4 Particulate matter

Particulate matter i.e. aerosol particles are solid or liquid airborne particles with a size range more than one nanometer ($= 10^{-9}$ m) to 100 μm. Over 100 μm particles are rarely discovered or the atmospheric lifetime of them is short because of the gravitational settling. (Jokiniemi and Kauppinen, 2002). According to Salonen and Pennanen (2007) particles can be divided into ultrafine particles ($d_P < 0.1$ μm), fine particles ($d_P < 2.5$ μm) and thoracic particles ($d_P <$

10 µm). Particles with $d_p > 10$ µm are super coarse particles. It appears to be that in combustion aerosol particles with $d_p < 1$ µm are fine particles and d_p 1-10 µm are coarse particles (Hytönen et al., 2008; Tissari, 2008).

Fine particle emissions can be divided into organic particles (POM, particulate organic matter), soot and ash particles. POM forms when flue gas cools down and unburned HCs condense into existing particles or form new particles by nucleation. POM emissions are exceptionally high during incomplete combustion. Soot is also referred to as elemental carbon (EC) or black carbon (BC). It is a product of a complicated reaction chain taking place in the diffusion flame where PAH compounds polymerize and form soot nuclei, which start to coagulate. Combustion of soot produces plenty of heat – problem is the unburned fraction. (FINE, 2013; Tissari, 2008.) BC has the greatest climate effect of all PM and Ramanathan and Carmichael (2008) claim that it is the strongest contribution to global warming after CO_2 emissions.

Ash is the incombustible inorganic mineral content of the wood fuel. Because it is not an actual product of combustion the formation of it cannot be prevented. In the cooling flue gas volatilized ash compounds go through gas-to-particle conversion (homogenous nucleation) and form fine fly ash particles which grow by coagulation and condensation. Typical fine fly ash compounds are different potassium-compounds, such as potassium sulphate (K_2SO_4), potassium hydroxide (KOH), potassium chloride (KCl) and potassium carbonate (K_2CO_3). In a good combustion even 90 % of PM_1 emissions is fine fly ash. (FINE, 2013; Tissari, 2008.) The release and composition of fine fly ash is dependent on temperature and amounts of different ash-forming elements. For example, Cl affects greatly on the release of K. (Knudsen et al., 2004.)

Coarse and super coarse particles from RWC are formed from non-volatilized ash which agglomerates. This so called bottom ash can also contain unburned char. Depending on the draught conditions and the structure of the combustion appliance coarse particles can eject into the flue gas and form the coarse fly ash fraction. (FINE, 2013; Tissari, 2008.)

The different particle formation mechanisms are put together in Figure 1.
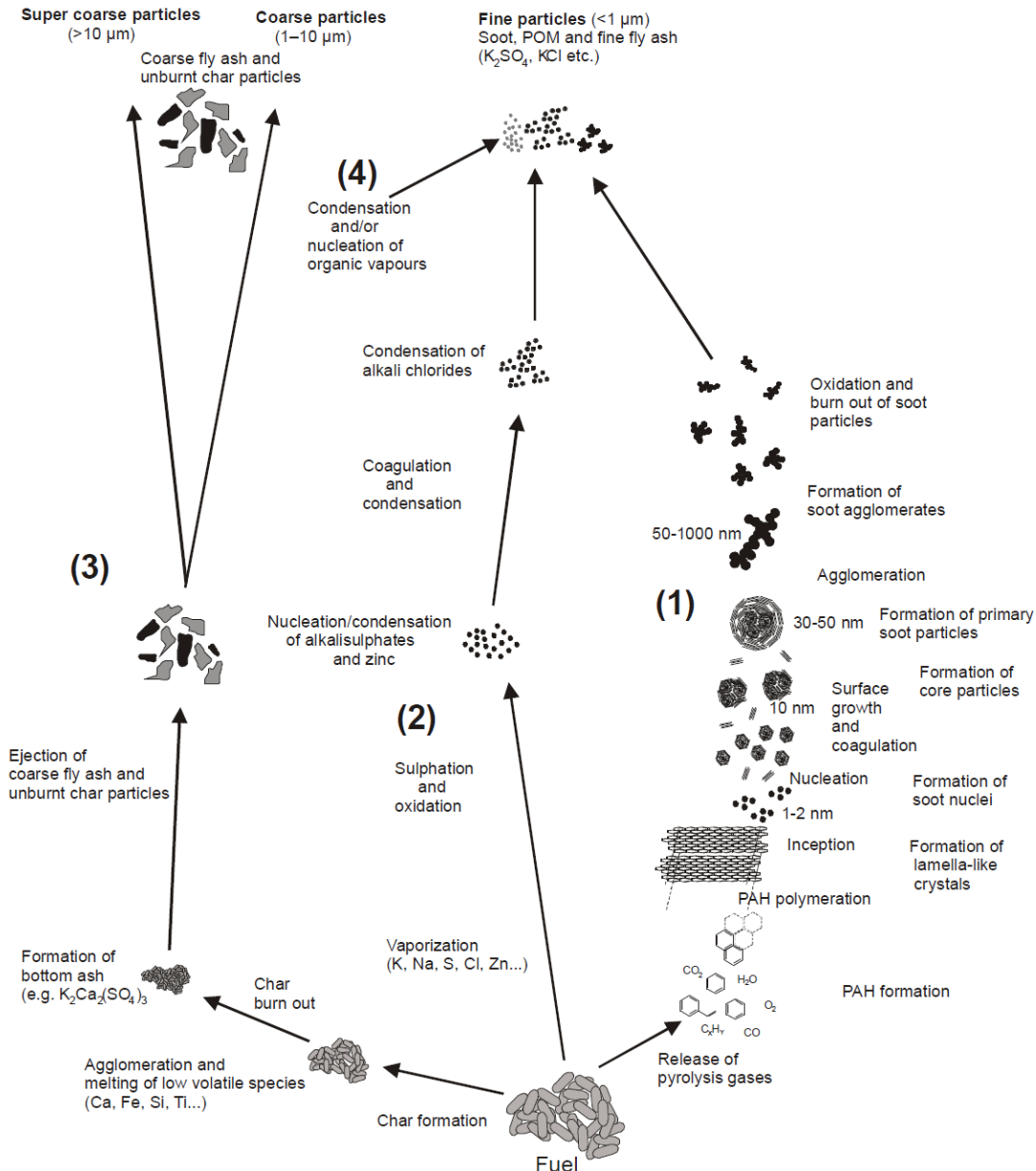
Figure 1. Formation of soot, particulate organic matter (POM), fine fly ash and coarse particles in residential wood combustion. (Tissari, 2008).

2.3 PARTICLE MEASUREMENTS FROM RWC

Measuring emissions from RWC is a challenge. Inside the furnace and stack the temperature is high and the amount of different vapours and gases varies. Particle size range is large and particles are different of a kind. If sample is diluted the flue gas eventually cools down. Organic compounds can occur in the gas phase or particle phase depending on the temperature which affects the saturation vapour pressure. This affects the PM concentration. Usually more than one measurement device is needed depending on what is measured:

particle concentration (number, size, mass), particle number and mass size distribution, particle chemical composition, particle morphology or gases and vapours. (Tissari, 2008.)

2.3.1 Sampling

When RWC flue gas is sampled, only a part of the flue gas (i.e. partial flow sampling) or all of the flue gas (i.e. whole flow sampling) is withdrawn from the stack usually via a probe/sampling tunnel. Sample is then transported to a measuring device (filter, collection plate or continuous electrical measuring device). (Hytönen et al., 2008.)

In the flue gas sampling PM losses on the walls of the tunnel are inevitable. Losses happen mostly due to electric forces, gravitation, thermophoresis, diffusion and inertial impaction. (Hytönen et al., 2008.) Thermophoresis is the movement of a particle to the direction of decreasing temperature and impaction happens in the curves of the tunnel because (large) particles are unable to follow the flow of the flue gas and thus, collide on the walls and attach to it (Hinds, 1999).

Isokinetic sampling is an important principle to follow in emission measurements, particularly when measuring total suspended particles (TSP). When sampling is isokinetic the flue gas velocity in the stack equals the flue gas velocity in the sampling tunnel and the gas flow directions are parallel. If sampling is not isokinetic it affects the particle sizes by increasing (sub-isokinetic, too low sampling velocity) or decreasing (super-isokinetic, too high sampling velocity) the share of large particles (in general $d_p > 1$ μm) in the sample. Isokinetic sampling is not a necessity when measuring RWC. In RWC PM_1 clearly dominate the PM emissions although combustion conditions vary this (Tissari, 2008). PM_1 practically behaves like a gas (i.e. the effect of inertia on it is small) and hence, isokinetic sampling is not needed for a PM sample to be representative. Furthermore, in batch combustion the flue gas velocity is overall quite slow and it varies according to the combustion cycle which would make isokinetic sampling difficult to execute. Finally, the loss of larger particles is not that big of a problem because smaller particle fractions ($PM_{2.5}$ and PM_1) are the main objects of interest anyway. (Hytönen et al., 2008.)

2.3.2 Sample treatment

PM measurements can be done without sample treatment, which means measuring TSP in the hot flue gas, or sample can be diluted with air. Dilution is needed because many PM measuring devices are sensitive to hot and humid flue gases with great PM concentrations. Dilution lowers flue gas temperature and partial pressures of vapours and gases drastically. This affects the concentration, size distribution and composition of PM especially in the beginning of combustion and during poor combustion when emissions of gaseous HCs are high. In other words dilution makes sample more representative for atmospheric conditions compared to primary emissions because of the condensation of organic species. Thus, the estimation of health and climate effects becomes more reliable. According to the engine standard ISO 8178 the condensation of organics is ensured when temperature below 52 °C is reached. In RWC this value should be treated with caution, however, because of numerous types of different organic species with different vapour pressures in the flue gas. The emissions of the most significant gaseous compounds (O_2, CO_2, CO, NO_x and gaseous HCs) are measured from hot and undiluted flue gas. Important factors in the dilution are the dilution ratio (DR) and effective mixing of the flue gases and the dilution air. (Hytönen et al., 2008.)

The effect of dilution on PM emissions is not entirely clear. Too small DR can potentially lead to overestimating the PM emissions and too high DR to underestimating them. In low dilutions (DR ≈ 20:1) PM mass concentration has been observed to increase but when the temperature of the sample has reached ambient levels (DR ≈ 350:1) the PM concentrations have dramatically reduced. The explanation to this is the evaporation of organic material in PM back to gas phase in order to maintain phase equilibrium. (Lipsky & Robinson, 2006.) In addition, the volatile species undergo several photochemical processes and oxidation in the atmosphere and result in the formation of secondary organic aerosol (SOA) and PM concentrations are increased again (Volkamer et al., 2006). Hereby, according to Lipsky & Robinson (2006), atmospheric levels of dilution (DR ≈ 10,000:1) should be applied if SOA formation is taken into account. In practice, sensitivity of measuring devices sets the limit for applied DR (Hytönen et al., 2008).

Dilution methods used in this thesis are presented in the section 4.3.1.

2.3.3 Measuring

In some European countries measuring standards for emissions from biomass combustion exist only for determining TSP. Standards are not available for dilution-based methods. (Hytönen et al., 2008.)

The desired particle property under interest defines the measurement method. Methods can be divided into off-line and on-line. In off-line the flue gas sample is collected to a sampling substrate, whether it is a filter, a collection plate in a conventional low-pressure impactor or a cyclone. The particle mass concentration or mass size distribution is then determined by weighing the substrate in question (gravimetric analysis). Afterwards it is possible to do different chemical and morphology analysis for the collected particles. Common sampling substrate materials are quartz filters, quartz wool, glass fiber filters, PTFE (polytetrafluoroethylene) i.e. Teflon filters, polycarbonate film and aluminium foils. The key to succeed in off-line methods is accurate weighing in controlled conditions where temperature and humidity can be adjusted. Sample storage should be done in dark and cold, for example, in a fridge. (Hytönen et al., 2008.)

On-line methods are comprised of different electrical continuous measuring devices, which utilize the physical properties of the particles and convert it into concentration (number, size, mass) or corresponding size distributions. The main benefit of the on-line methods is the possibility to find out how the emissions behave and develop during the combustion which is not possible with the off-line methods. (Hytönen et al., 2008.)

The sample treatment for chemical characterization is defined by the analysis in question. Different extraction treatments are common. In chemical analysis PM can be divided into carbonaceous and inorganic matter. Carbonaceous can be divided further into OC (organic carbon) and EC i.e. soot or BC which is the light-absorbing fraction of carbon. OC contains numerous of different organic compounds and can be separated into water-soluble and water-insoluble fractions. Inorganic matter contains all the non-carbonaceous compounds like different alkali salts and trace metals. (Hytönen et al., 2008.)

3. THE AIMS OF THE WORK

The aims of the thesis were to characterize the PM and gaseous emissions formed in batch-wise operated Finnish modern masonry heater and to test a novel sampling method for PM. The obtained results of the continuous measurement devices, filter collections and three different PM sampling methods (reference sampling method, novel sampling method and TSP) were compared between each other and legislation. Also the usability of the novel sampling method was evaluated.

4. MATERIALS AND METHODS

4.1 COMBUSTION APPLIANCE AND COMBUSTION SETTINGS

The combustion appliance used in the measurements was a modern masonry heater (MMH) made of soapstone (weight 1280 kg, dimensions $0.85 \times 0.61 \times 1.44$ m^3). Primary air is fed under the grate and comprises 10 % of the total combustion air flow. Other air stages are window flushing air and secondary air which comprise 40 % and 50 % of the total combustion air, respectively. The location of the window flushing air feed is on the front edge of the furnace, secondary air on the top of the furnace. The nominal energy output of the MMH is 1.6 kW. In the result section the appliance is abbreviated to TS-MMH.

The operating of the MMH was standardized throughout the measurements. The wood fuel was Finnish birch with moisture content approximately 10-15 % by weight. Batches were weighed with Sartorius CP 34001P High Capacity Digital Weighing scale and each batch was 3.0 kg $\pm$ 0.010 kg. The ignition batch had 10 pcs of medium sized logs (0.25 and 0.30 m) and 4-6 pcs of smaller pieces of wood and birch bark which were used to ignite the batch. Ignition was done from the top of the batch and external metal rack was used to keep the batch from collapsing. New batches were added when CO_2 concentration in the undiluted flue gas dropped to 4.0 %. Each additional batch had 6 slightly larger logs in it. Before adding the batch the char bed was gently shuffled and spread on the grate evenly. The draught was always maintained stable (12 $\pm$ 2 Pa) with the flue gas fan. If measurements were carried out on consecutive days the MMH was cooled down overnight with fans to ambient temperature.

Figure 2. The wood fuel batches. On the right is the ignition batch placed into the furnace.

The mass of the bottom ash was determined in experiments 5, 13 and 14. Ash was collected from the ash dump to small plastic bags and weighed with Sartorius CP 34001P High Capacity Digital Weighing scale. The ash content of the wood fuel was approximately 0.7 % by dry weight but this is not entirely accurate because the ash contained also small amounts of unburned char.

4.2 GAS AND TEMPERATURE MEASUREMENTS

Gaseous samples of the raw flue gas were taken straight from the stack with an insulated sample line which was heated up to 180 °C to prevent the condensation of the compounds. Sample line had a ceramic filter which was used to remove the particles.

Two gas analyzing systems were used in parallel. The gas analyzing rack (ABB Hartman & Braun) had a combination of different measurement technologies in it. O_2 was measured based on paramagnetism, CO and CO_2 on infrared spectroscopy, NO_x on UV-spectrometry and organic gaseous compounds (OGC) were measured with flame ionization detector (FID). The data was collected with data acquisition system. In addition, Gasmet[TM] DX-4000 Multicomponent fourier transform infrared spectroscopy (FTIR) Gas Analyzer was used. The main compounds of interest were O_2, CO_2, CO, NO_x and vaporous H_2O but device was also calibrated for 28 different HCs. Concentration of O_2 was measured using a separate ZrO_2 cell integrated into the device. Otherwise the function of DX-4000 rested on FTIR spectroscopy. Sample analyses and data logging was done with an external computer with CALCMET-software.

In FTIR spectroscopy sample continues from stack to the device through a heated line. Infrared radiation is passed through the gas sample where part of the radiation is absorbed, part of it passes through the sample to the detector. Each component absorbs radiation on specific frequencies and the composition and quantity of different compounds can be solved from the resulting spectrum. The Fourier transform is needed for decoding the individual frequencies and it is performed by the computer. (Thermo Nicolet Corp., 2001.)

FID is a sensitive gas chromatographic detector. Sample is delivered to a H_2 flame with N_2 or some other inert carrier gas. In the flame charged particles (ions and electrons) are created from carbonaceous compounds in the sample. The amount of particles produced in the H_2 flame itself is minor. Particles continue to two electrodes where an electric potential is applied. With the help of particles this potential creates an electric current which is measured by an electrometer. The intensity of the current is directly proportional to the amount of created particles and finally, to the mass flow of carbon. (Zachowski and Paleologos, 2009.)

In the reference sampling method (section 4.3) the hot flue gas temperature was measured with K-type thermocouple in the stack before the porous tube diluter (PRD). Data collection was done with National Instruments cDAQ-9172 data acquisition system (input models NI 9211 and NI 9203). System was connected to a computer and data was logged with NI LabVIEW SignalExpress software. For calculating the dilution ratio and making the temperature correction (section 4.8) the CO_2 concentration and the temperature in the diluted sample were measured after ED using Vaisala CARBOCAP® Carbon Dioxide Probe GMP343 which was connected to a computer.

In the novel sampling method (section 4.4) the CO_2 in the diluted sample was measured after the mass flow meter using ABB A02040 Uras 14 Gas Analyzer. K- and S-type thermocouples were used to measure temperature from the dilution air, flue gas, PRD (2 pcs inside, 2 pcs outside) and from the sampling line before and after filter. CO_2 and temperature data was collected with National Instruments cDAQ-9172 data acquisition system (input models NI 9211 and NI 9203) and logged with NI LabVIEW SignalExpress software.

4.3 REFERENCE SAMPLING METHOD

4.3.1 Particle sampling and dilution

The partial flow sample was diluted in two stages. The sample was taken from the stack straight through PRD followed by ejector diluter (ED) which, in addition to dilution, ensured the proper mixing of the flue gas with dilution air. Dilution air was in room temperature, dried and filtered in the pressure station (TSI Inc.). The flow of the dilution air (18 lpm for PRD, 50 lpm for ED) was adjusted with GFM mass flow controller (Aalborg Instruments & Controls, Inc.). After ED the sample flow continued to a metal probe and was separated to continuous measurement devices and filters. The sample flow was maintained with vacuum pumps. The goal was to sustain the DR between 40-50. This sampling arrangement was developed by Tissari et al. (2007) and is presented in Figure 3.
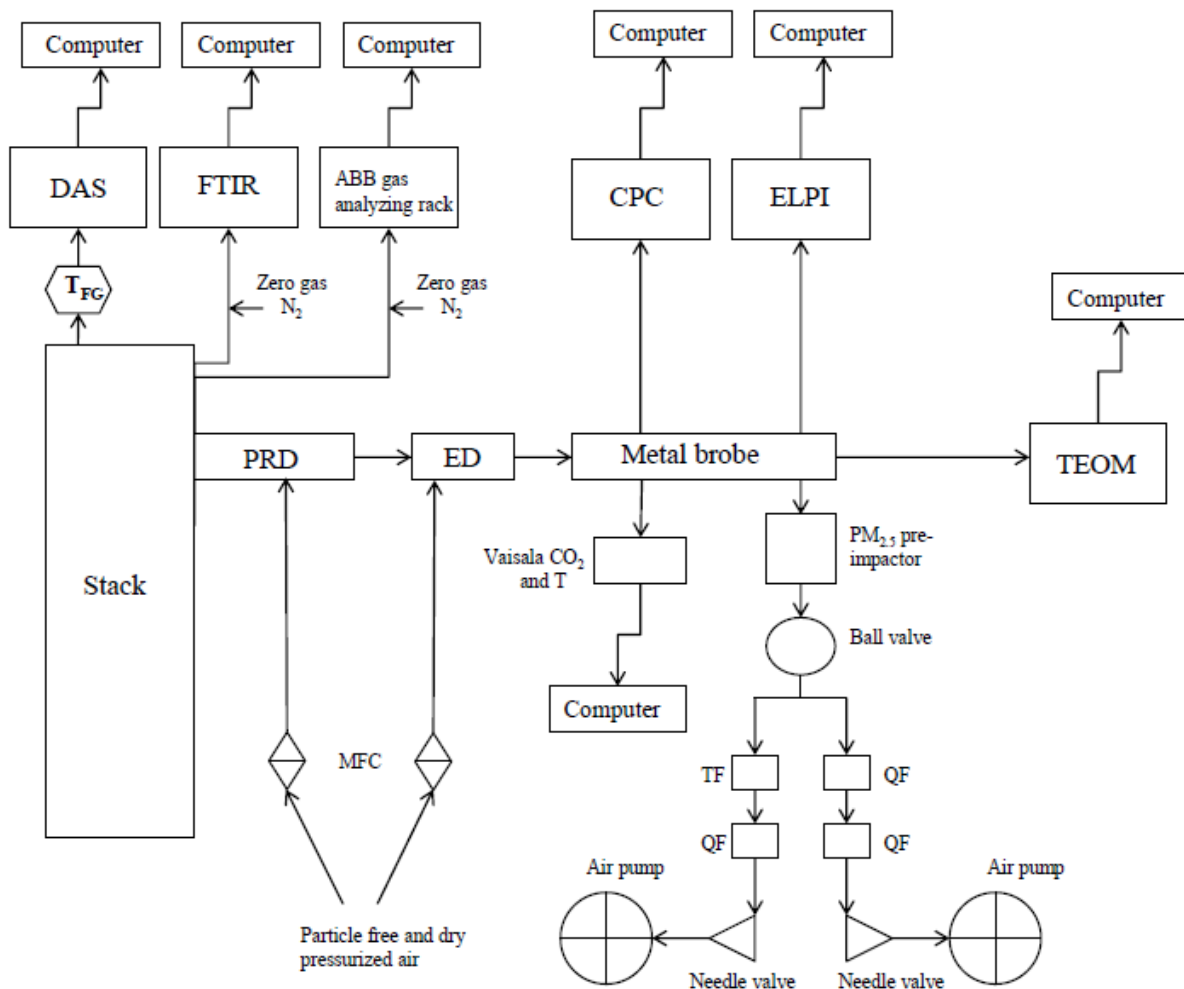
Figure 3. Schematics of the reference sampling method measurement arrangement. MFC, mass flow controller; T_{FG}, flue gas thermocouple; DAS, data acquisition system; TF, teflon filter; QF, quartz filter.

In Figure 4 is a schematic picture of a combination of PRD and ED. In PRD dilution air flows through pores with a diameter of approximately 20 µm which exist throughout the inner side. In ED the dilution air flows in with pressure around the ejector nozzle causing a pressure drop, which drags the sample through the nozzle and mixes it effectively with the dilution air.
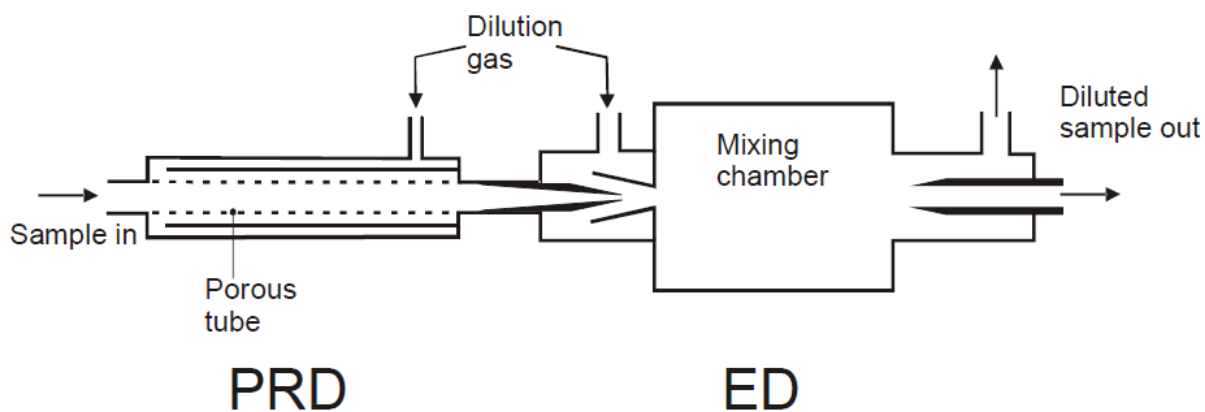
Figure 4. Combination of porous tube diluter (PRD) and ejector diluter (ED). (From Hytönen et al., 2008.)

4.3.2 Particle number and number size distribution measurements

The total real-time particle number concentration measurements were carried out with Condensation Particle Counter (CPC), TSI Model 3775. The smallest detectable particle for this model is 4 nm in diameter and maximum particle concentration is 10^7 cm^{-3}. The idea with CPC is to grow the particles so they can be observed optically. In the Model 3775 the particles are grown with butanol vapour. The sample stream is led through heated saturator (39 ° C) where butanol vaporizes and diffuses into sample stream. This mixture flows through cooled condenser (14 °C) where butanol vapour becomes supersaturated and condenses on the surface of the particles. The sample stream is then introduced to light and the grown particles are counted with an optical detector. The particle concentration determines which operation mode is in use. Single particle counting, when individual pulses are counted, is utilized when particle number concentration is smaller than 50,000 cm^{-3}. When concentration exceeds this the photometric operation mode switches on. In this case the total light scattered is detected and the intensity is compared with calibration levels. Sample flow is created with an internal pump. In these measurements the flow rate was 1.5 lpm to minimize the transport losses and to have a shorter response time (4 s). Inside the device was an internal critical orifice controlling the sample flow. Time resolution for each measurement was 1 second. CPC was

connected to an external computer and data was logged with Aerosol Instrument Manager - software.

Electrical Low Pressure Impactor (ELPI^{TM}, Dekati Ltd.) was used to determine the real-time particle number size distribution. ELPI consists of an unipolar corona charger, low pressure cascade impactor and multi-channel electrometer. The size range of ELPI is 30 nm to 10 μm, with filter stage 7 nm to 10 μm. In this study the filter stage was in use, the sample flow rate was 10 lpm and measurement time resolution was both 5 and 10 seconds. External computer with ELPIVI 4.0 -software was used for data logging.

The sample stream flows through the inlet into the 5 kV corona charger which produces ion flow of 1 μA. This flow charges particles into known unipolar charge level. Inside the corona exists a static trap field which is formed with a voltage of 400 V. Trap field removes the charged molecule groups and particles smaller than the cutoff diameter of the lowest stage. When the filter stage is used, the trap field must be turned off. Field removes also some larger particles but this loss is compensated with the charger efficiency function. After the charger the sample stream enters the low pressure (100 mbar) impactor with 13 electrically insulated stages and sintered collection plates coated with 1 μl of vacuum oil. Stages are connected to an electrometer current amplifier. The structure of the impactor assembly is such that the sample stream accelerates and makes sharper turns towards the end. Larger particles are unable to follow the flow and are collected to the impactor stages according to their aerodynamic diameter while smaller particles continue in the stream. The collected particles donate their charges and induce an electrical current which is detected by a sensitive multi-channel electrometer. The value of the current in each channel is directly proportional to the number of particles.

4.3.3 Particle mass measurements

TEOM (tapered element oscillating microbalance) is a device for measuring real-time particle mass concentration. The particle sample is collected on a filter which is located in the free end of a shallow and narrowing tube whereas the other end of the tube is rigid and attached to the device. The free end of the tube is oscillated at its resonance frequency which is strongly dependent on tube's mass. As the particles deposit on the filter, its mass increases and the

oscillating frequency decreases. The change in the frequency combined with the sample volume is converted to particle mass concentration. (Patashnick et al., 2002.)

The tapered element device used in this study was Thermo Scientific™ TEOM Series 1405 Ambient Particulate Monitor which is a common device when measuring ambient outdoor air. Applied filters were 13 mm Pallflex TX40. Device can be adjusted to measure PM_{10}, $PM_{2.5}$, PM_1 or TSP. The maximum concentration for Series 1405 is 1 g m^{-3}, measurement resolution 0.1 µg m^{-3} and sample temperature operating range from -40 °C to 60 °C. In this study the total PM was measured although losses surely occurred in the sampling line. The flow rate used was 1.0 lpm and maintained with an external pump. Measurement time resolution was 10 seconds and the temperature of the tapered element was 35 °C on average. The device had an internal data logging system and data was collected later via USB port.

The filter samples were collected using a cascade pre-impactor with two stages. First stage cut out the particles larger than 10 µm, second particles with the diameter of 2.5-10 µm. The pre-impactor stages had aluminium foils as collection plates with a diameter of 25 mm. The foils were coated with a mixture of Apiezon-L grease and toluene to minimize the particle bounce. The pre-impactor was sized for the flow rate of 20 lpm. After the pre-impactor the $PM_{2.5}$ samples were collected on two parallel lines in a filter holder. Samples for gravimetric analyzes were collected on 47 mm PTFE-filters and samples for OC and EC analyzes were collected on 47 mm quartz fiber filters. Both lines had a quartz fiber backup filter for collecting gaseous OC. Purpose of this was to get correct particle mass by subtracting the mass of gaseous OC after the PTFE-filter from the mass of total carbon on the front quartz filter. Both sampling lines had their own pump with a flow rate of 10 lpm. After the sampling the filters were placed in a Petri dish sealed with PARAFILM® and stored in a fridge.

The filters were weighed before and after sampling with Mettler Toledo MT5 Micro Balance with accuracy of 1 µg. Before each weighing the filters were stabilized in the weighing room for 24 hours. During experiments 11 and 13 weighed aluminium foils were used in the pre-impactor for measuring the mass concentration of larger particles.

4.3.4 Particle chemical composition

Particle OC and EC concentrations were determined using thermal-optical method. Analyzes were done using Sunset Laboratories Inc. carbon analyzer. The separation of OC and EC is based on the different optical properties of the carbon fractions: EC absorbs light, OC does not.

The quartz filter is placed in the oven of the thermal-optical device. First the filter is heated to 850 °C in a completely oxygen-free and inert helium atmosphere which causes desorption of OC from the filter. Next the vaporous OC flows through MnO_2 oven and is catalytically oxidized to gaseous CO_2 and then reduced to CH_4. Helium stream transports this CH_4 to FID where the amount of it is measured. EC goes through same process with the exception that the desorption takes place in oxidizing He/O_2 atmosphere and in lower temperature. Later temperature is again raised to about 940 °C. During the first heating of the filter some of the OC is pyrolytically converted to EC which could lead to overestimating the share of EC. This is corrected by continuously observing the OC-to-EC -conversion with laser light passed through the filter and measuring changes in the laser's absorbance. (NIOSH, 1999.)

4.4 NOVEL SAMPLING METHOD

4.4.1 Particle sampling and dilution

The partial sample was taken with PRD attached to the stack. The dilution air came from the pressure station (TSI Inc.). Applied DR was 20. Needle valve was used to adjust the dilution and pressure over the valve was monitored with Keller LEO 2 digital manometer (Serpens Inc.). In addition, critical orifice was positioned before PRD and in the end of the sampling line to keep the sample flow steady. The arrangement schematics can be found from Figure 5.
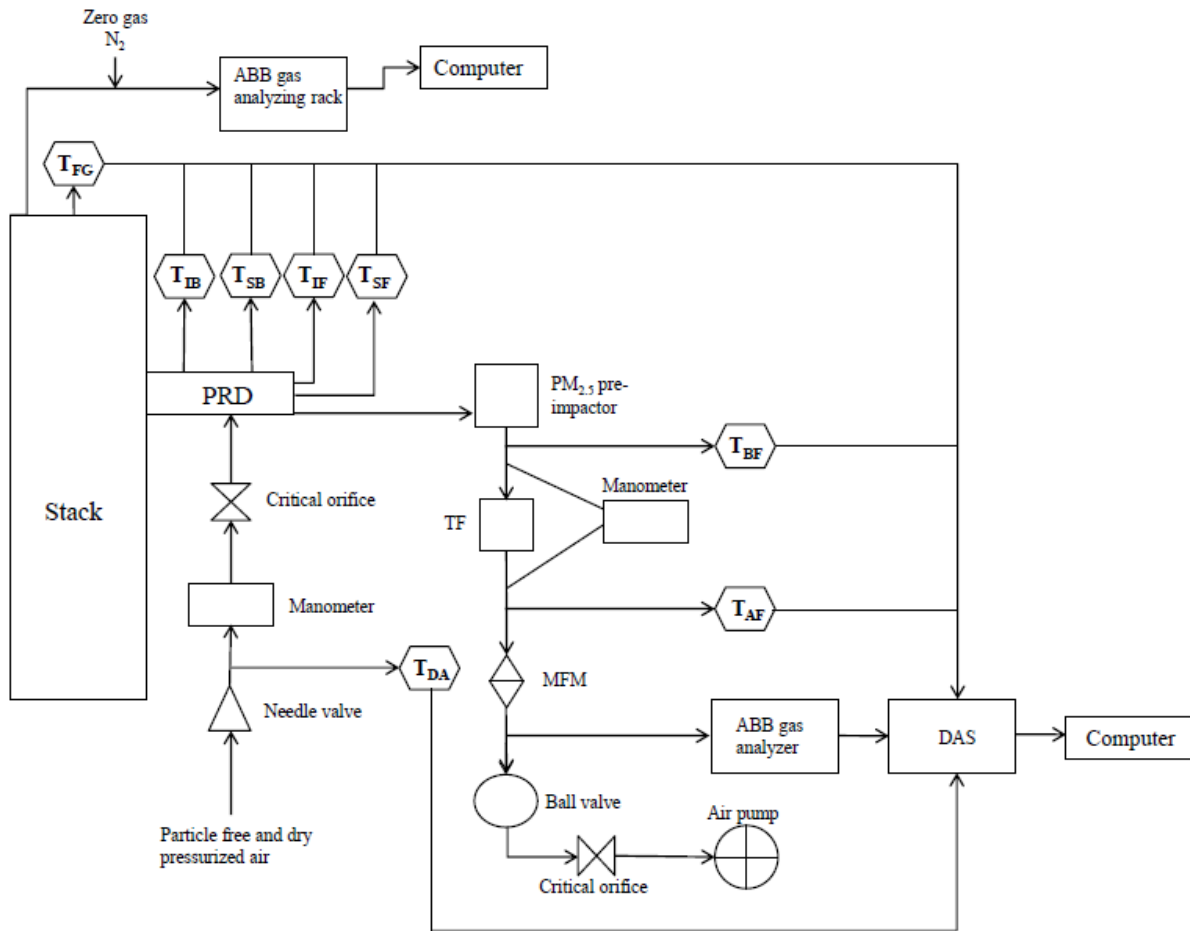
Figure 5. Schematics of the novel sampling method. T_{DA}, dilution air thermocouple; T_{FG}, flue gas thermocouple; T_{IB}; inside back thermocouple; T_{SB}, surface back thermocouple; T_{IF}, inside front thermocouple; T_{SF}, surface front thermocouple; T_{BF}, before filter thermocouple; TF, teflon filter; T_{AF}, after filter thermocouple; MFM, mass flow meter; DAS, data acquisition system.

4.4.2 Particle mass measurements

The samples were collected to 90 mm Zefluor® PTFE Membrane Filter placed in a filter holder. Larger particles were removed with EPA WINS $PM_{2.5}$ separator with 37 mm glass fiber filter in it (Figure 6). Sample flow rate (16.7 lpm) was created with an air pump and monitored with TSI Inc. 4100 Series mass flow meter. The increased particle load on filter caused a pressure drop and because of this a valve was positioned in the end of the sampling line in order to adjust the flow. Monitoring of the pressure difference before and after filter was done with Thommen HM 35 Digital Manometer. After the sampling the filters were placed in a plastic Petri dish sealed with PARAFILM® and stored in a fridge.

The 90 mm filters were weighed before and after sampling with Sartorius CPA1245 with accuracy of 0.1 mg. The stabilizing time before each weighing was 24 hours. Weighed glass fiber filters were used in the $PM_{2.5}$ separator for measuring the mass of larger particles only in experiments 10 and 11 (section 4.6). The scale used was Mettler Toledo MT5 Micro Balance.

Figure 6. Filter holder and $PM_{2.5}$ separator used in the novel sampling method.

4.5 TOTAL SUSPENDED PARTICLES

TSP measurements were conducted according to European Standard EN 13284-1. Method is primarily developed for measuring PM emissions in power plants where flue gas velocities are higher. A specific sampling probe heated to 160 °C was used to take the partial sample form the stack. On the other end of the probe was a 47 mm quartz filter where the samples were collected. Flow rate varied between 3-10 lpm. Filters were weighed by Symo Inc., Kuopio.

4.6 MEASUREMENT MATRIX

The measurement matrix for filter collections is presented in Table 1. Continuous devices measured the whole combustion in every experiment. In experiments 1-9 the first filter collection was done during the first batch. After the collection ($CO_2 < 4$ %) new filters were placed, new batch was added and sampling of the second and the third batch was done on the same filter.

Table 1. Measurement matrix for filter collections in the novel sampling method, reference sampling method and TSP method.

Experiment number	Sampling target	Novel sampling	Novel sampling DR	Reference sampling	TSP
1	1. batch, 2. + 3. batch			x	
2	1. batch, 2. + 3. batch			x	
3	1. batch, 2. + 3. batch			x	
4	1. batch, 2. + 3. batch			x	
5	1. batch, 2. + 3. batch			x	
6	1. batch, 2. + 3. batch			x	
7	1. batch, 2. + 3. batch			x	
8	1. batch, 2. + 3. batch			x	
9	1. batch, 2. + 3. batch			x	
10	2. batch	x	20	x	x
11	2. batch	x	20	x	x
12	2. batch	x	20	x	x
13	the whole combustion			x	x
14	the whole combustion			x	x
15	the whole combustion			x	x

4.8 CALCULATION OF DR AND EMISSION FACTORS

4.8.1 Dilution ratio

All the nominal particle emission values were multiplied with DR which was monitored continuously by measuring the concentrations of CO_2 from both undiluted and diluted flue gas. DR was calculated with Equation 1 (Tissari, 2008).

$$DR = \frac{CO_{2,FG} - CO_{2,BG}}{CO_{2,D} - CO_{2,BG}} \qquad (1)$$

where

$CO_{2,FG}$ = CO_2 concentration in dry and undiluted flue gas
$CO_{2,D}$ = CO_2 concentration in the diluted flue gas
$CO_{2,BG}$ = CO_2 concentration in the background dilution air (400 ppm = 0.04 %)

4.8.2 Air-to-fuel ratio

Air-to-fuel ratio (λ) describes how much extra air was present in the combustion. It was calculated with Equation 2 according to SFS 5624.

$$\lambda = \frac{20.96}{20.96 - E_M} \qquad (2)$$

where

E_M = dry and undiluted flue gas O_2 concentration (%)
20.96 = ambient air O_2 concentration (%)

4.8.3 Temperature correction

Temperature affects the volume of the flue gas and thus, the concentration of emissions. To make the results comparable all the results were presented in normalized cubic meter (Nm^3). The measured emission values were normalized according to the reference temperature with Equation 3.

$$c_{RT} = c_M \frac{T_M}{T_{RT}} \qquad (3)$$

where

c_{RT} = concentration in reference temperature
c_M = measured concentration value in dry flue gas (mg m^{-3} or # cm^{-3})
T_M = measured temperature of the diluted sample (K)
T_{RT} = reference temperature (0 °C = 273.15 K)

4.8.4 Nominal emission value in relation to a volume of flue gas

Emission values in a certain volume of dry flue gas were normalized into 13 % O_2 concentration which is a long-time average value in the batch combustion of wood. Normalization was done according to SFS 5624 by multiplying the measured emission values (c_m) with oxygen reduction factor r (Equation 4).

$$r = \frac{20.96 - O_{2,N}}{20.96 - O_2} \qquad (4)$$

where

20.96 = ambient air O_2 concentration (%)
$O_{2,N}$ = O_2 concentration in dry flue gas used in the normalization (13 %)
O_2 = dry and undiluted flue gas O_2 concentration (%)

4.8.5 Nominal emission value in relation to energy input

Calculations of the nominal emission values (mg MJ^{-1}) were done according to Equation 5 (SFS 5624).

$$q_e = c_M \times \lambda \times k \times Q_s \tag{5}$$

where
q$_e$ = nominal emission value (mg MJ^{-1})
c$_M$ = measured emission value in dry flue gas (mg m^{-3} or # cm^{-3})
λ = air-to-fuel ratio
k = fuel moisture factor (1.02 in all calculations)
Q$_s$ = volume of dry flue gas in the reference conditions in relation to energy unit in the combustion of dry fuel (0.25 m^3 MJ^{-1} in all calculations)

4.8.6 Fuel moisture factor

The fuel moisture content lowers the heating value of the wood fuel because the evaporation of water consumes heat energy. This latent heat lowers the combustion temperature which leads to lower combustion temperatures and increased emissions. This is why fuel moisture factor (k) needs to be applied in the Equation 5. It was calculated according to SFS 5624 as follows.

$$k = \frac{H_u}{H_u - H_w} \tag{6}$$

where

k = fuel moisture factor
H$_u$ = the net heating value of dry fuel (18.5 MJ kg^{-1} for wood)
H$_w$ = the amount of heat consumed in water evaporation (MJ kg^{-1})

H_w (approximately 0.38 MJ kg^{-1}) was calculated with Equation 7 (SFS 5624).

$$H_w = w_v \times l_v = \frac{\gamma_v}{1-\gamma_v} \times l_v \qquad (7)$$

where

w_v = the mass ratio of water and dry substance
l_v = the evaporation heat of water (2.5 MJ kg^{-1} in 0 °C)
γ_v = the mass ratio of water and wet fuel (0.132)

5. RESULTS AND DISCUSSION

5.1 GASEOUS EMISSIONS

Gaseous compounds were measured simultaneously with two gas analyzers. The main compounds of interest were O_2, CO_2, CO, NO_x, vaporous H_2O and different gaseous HCs. The detailed average emissions are presented in Appendix I. The standard deviations describe the deviation between the experiments.

The time series of O_2, CO_2 and CO concentrations can be seen in Figure 7. The cyclic process is typical for batch combustion. When the new batch was added the CO_2 concentrations rose and O_2 concentrations went down.
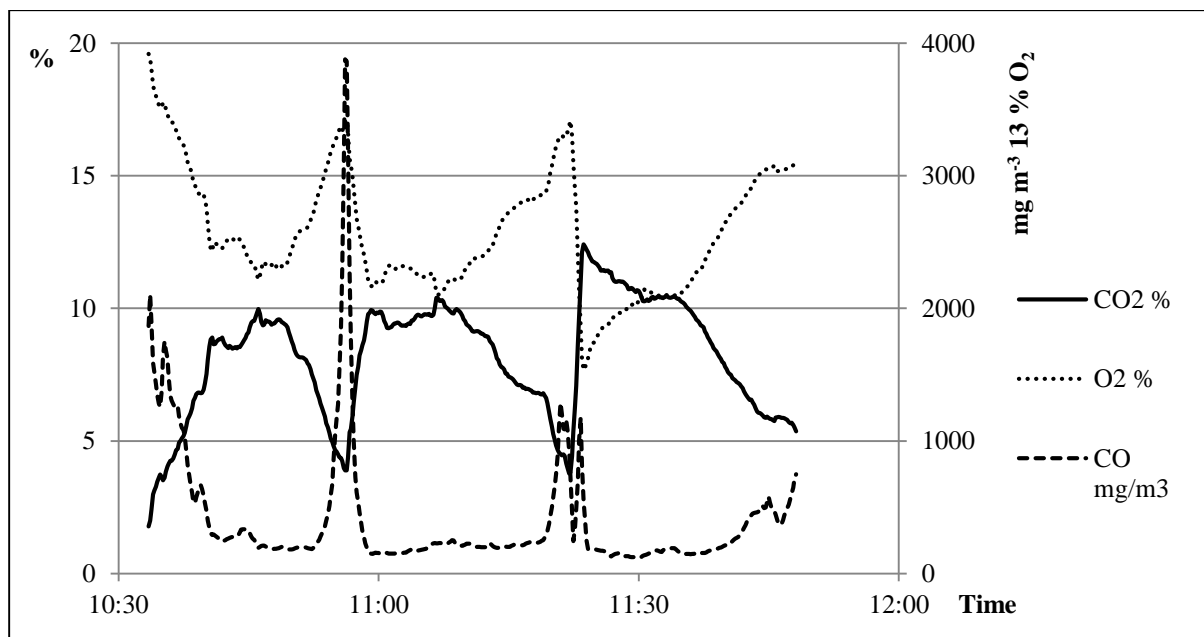

Figure 7. Experiment 2 time series of oxygen and carbon dioxide as flue gas volume percentages as measured with ABB gas analyzing rack and concentration of carbon monoxide as measured with FTIR.

The average CO concentrations were highest during the first batch whereas emissions of NO_x were quite stable throughout the combustion (Figures 7 and 8). Usually the adding of the second batch caused a high and short peak in the CO emissions (Figure 7). The variations of CO and NO_x emissions from the first batch were 688-1505 mg m^{-3} and 84-356 mg m^{-3}, respectively. During the beginning of char burnout the emissions of CO started to go up again

(Figure 7). This was due to the low diffusion rate of O_2 to the char bed and the cooling of the furnace which was caused by the high volume of excess combustion air (Tissari, 2008).
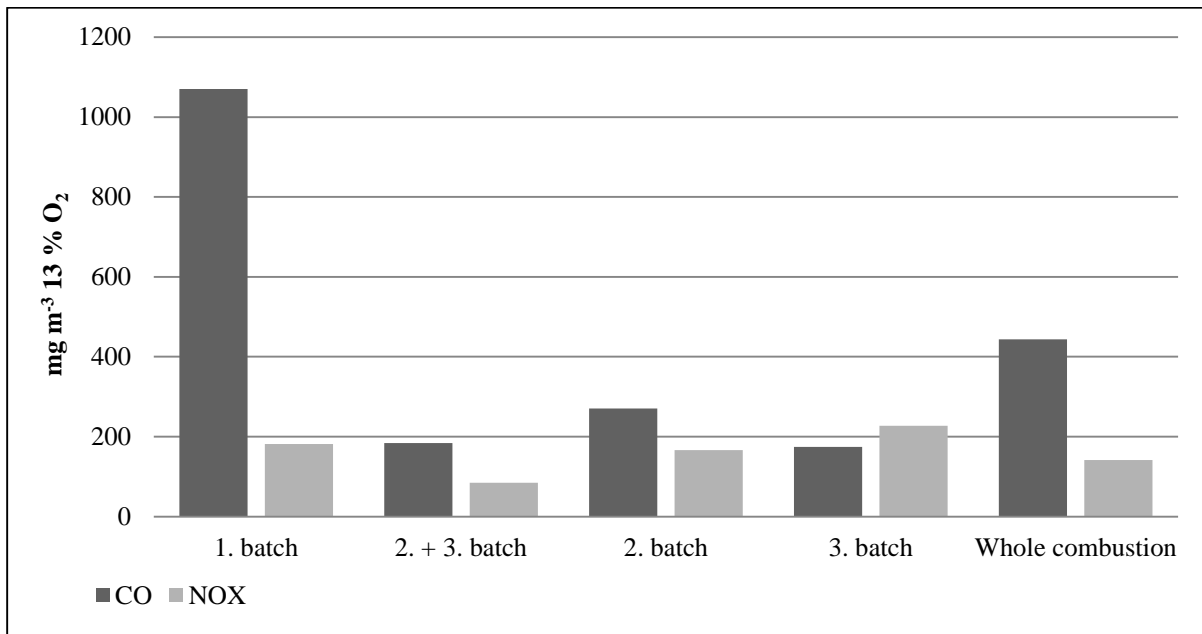
Figure 8. Average concentrations of carbon monoxide and nitrogen oxides in different combustion phases as measured with FTIR.

OGC and CH_4 emissions were high only during the first batch (Figures 9 and 10) with variations of 22-208 mg m^{-3} and 10-55 mg m^{-3} in the first batch, respectively. A clear but short peak occurred commonly in both, the OGC and the CH_4 emissions, when the second batch was added and combustion conditions became temporarily poor (Figure 10).
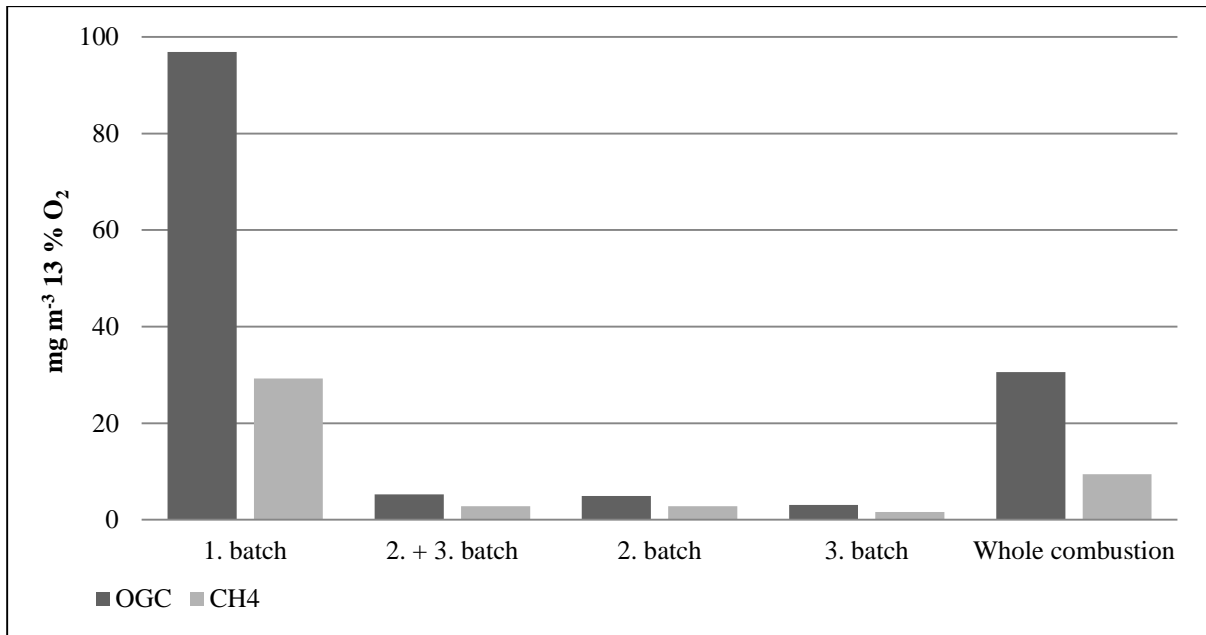
Figure 9. Average concentrations of organic gaseous compounds and methane in different combustion phases. OGC measured with FID, methane with FTIR.
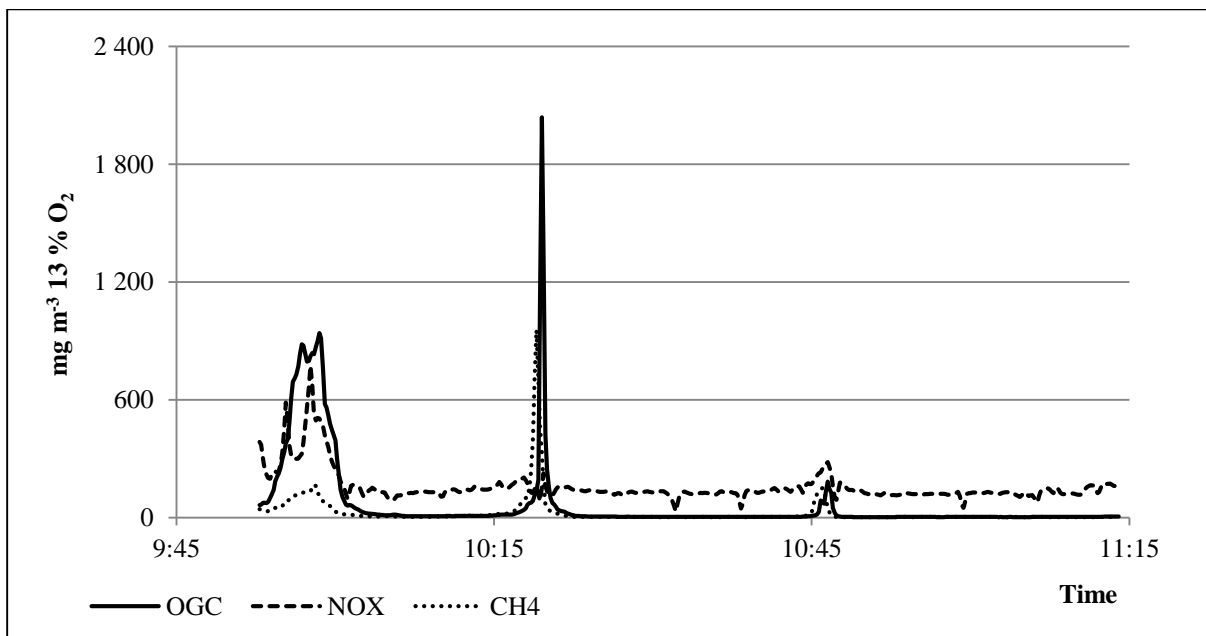

Figure 10. Experiment 6 time series of organic gaseous carbon, nitrogen oxides and methane concentrations. OGC measured with FID, NO_x and CH_4 with FTIR.
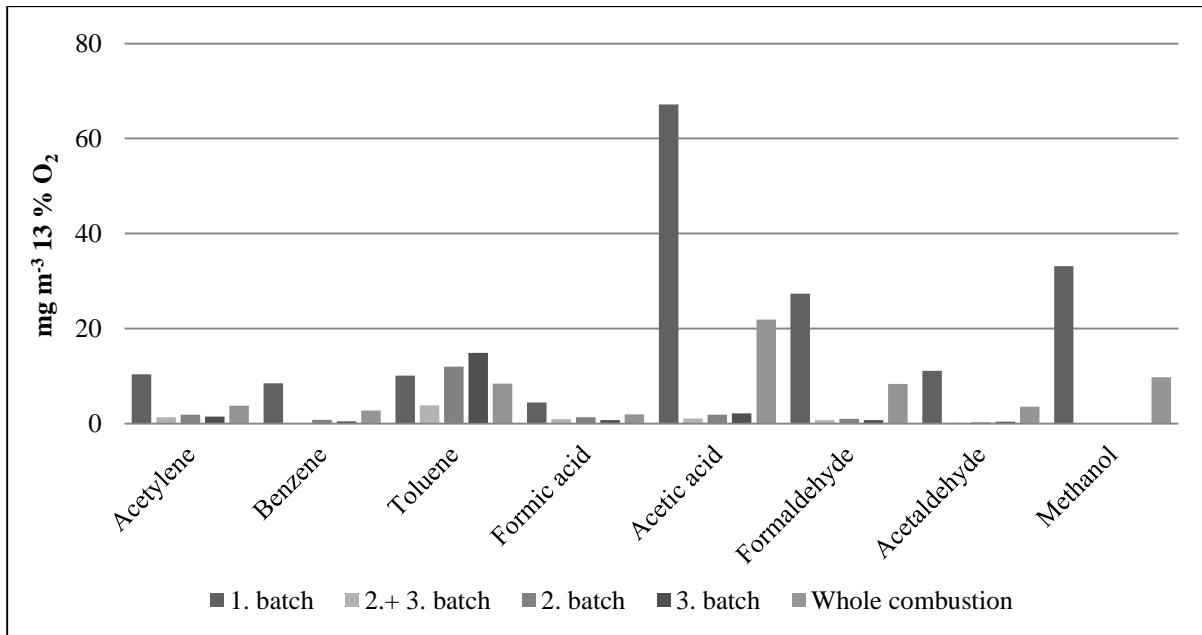
Figure 11. Average concentrations of hydrocarbons in different combustion phases as measured with FTIR.

Eight most common hydrocarbons were chosen to further analysis (Figure 11). Acetic acid had the highest concentration peak but concentrations were significant only during the first batch. Toluene, instead, kept forming throughout the combustion and the concentrations of it increased towards the end.

OGC emissions from TS-MMH were practically same than the ones from MMH in Tissari et al. (2008a) and clearly lower compared to other appliances (Table 2). In addition of low OGC emissions the best quality of TS-MMH was very low CO emissions. NO_x emissions from TS-MMH were quite similar to those from other appliances.

Table 2. Comparison of the whole combustion average OGC, CO and NO_x emission factors between different studies and combustion appliances. MMH, modern masonry heater; CMH, conventional masonry heater; SS, sauna stove; PB, pellet boiler.

Emission parameter	This study	Tissari et al. (2008a)			Tissari et al. (2008b)	Tissari et al. (2007)		Lamberg et al. (2011)
	MMH	MMH	CMH	SS	CMH	MMH	CMH	PB
OGC (mg MJ^{-1})	21	22	148	546	120	nda	126	nda
CO (mg MJ^{-1})	240	765	1202	3005	2295	1530	2022	63
NO$_x$ (mg MJ^{-1})	61	nda	nda	nda	77	49	55	81

nda, no data available.

Very low HC emissions are clearly an advantage of TS-MMH (Table 3) but it has to be kept in mind that applied measurement methods differ between the studies and might have affected the results.

Table 3. Comparison of the whole combustion average gaseous hydrocarbon emission factors (mg MJ^{-1}) between this study, Tissari et al. (2007) and Hedberg et al. (2002). MMH, modern masonry heater; CMH, conventional masonry heater; SS, sauna stove; WS, wood stove.

Hydrocarbon	This study	Tissari et al. (2007)		Hedberg et al. (2002)
	MMH	CMH	SS	WS
CH$_4$	6[c]	25[c]	218[c]	nda
Acetylene	2[c]	7[c]	96[c]	nda
Benzene	1[c]	25[c]	137[c]	82[a]
Toluene	3[c]	7[c]	32[c]	40[a]
Formic acid	1[c]	nda	nda	nda
Acetic acid	9[c]	39[c]	22[c]	nda
Formaldehyde	5[c]	20[c]	39[c]	23[b]
Acetaldehyde	2[c]	12[c]	12[c]	5[b]
Methanol	5[c]	16[c]	9[c]	nda

nda, no data available
[a] measured using BTX-monitor
[b] sampled using DNPH-Silica Cartridges, measured with HPL-chromatography
[c] measured using FTIR

5.2 PARTICLE EMISSIONS

Particle mass concentrations, particle number concentrations and particle number size distributions were measured with different continuous on-line measuring devices and off-line sampling methods. Particle chemical composition was determined later from collected filter samples. The detailed average emissions are presented in Appendix II. The standard deviations describe the deviation between the experiments.

The PM$_{2.5}$ concentrations varied significantly between the combustion phases. The highest particle mass concentrations were formed during the first batch most likely due to the cold furnace which consumed heat to warm up. The results of the reference sampling filter collections in experiments 1-9 can be found from Figure 12. The average PM$_{2.5}$ concentration of the first batch (184 mg m^{-3}) was about 2.5-fold higher than the average concentration during the second and the third batch (75 mg m^{-3}). The average PM$_{2.5}$ concentrations during the second batch and the whole combustion were 79 mg m^{-3} and 113 mg m^{-3}, respectively (Figures 13 and 14). The high concentrations during the first batch cannot be seen in the whole combustion average concentrations so the separate sampling of the first batch was certainly necessary. Even though the sampling was carried out in the same way in every experiment and operating of the MMH was standardized some variation can be seen in the

results. For example, the concentration during the second and the third batch in the experiment 7 is about 2.3-fold to the one in the experiment 6.
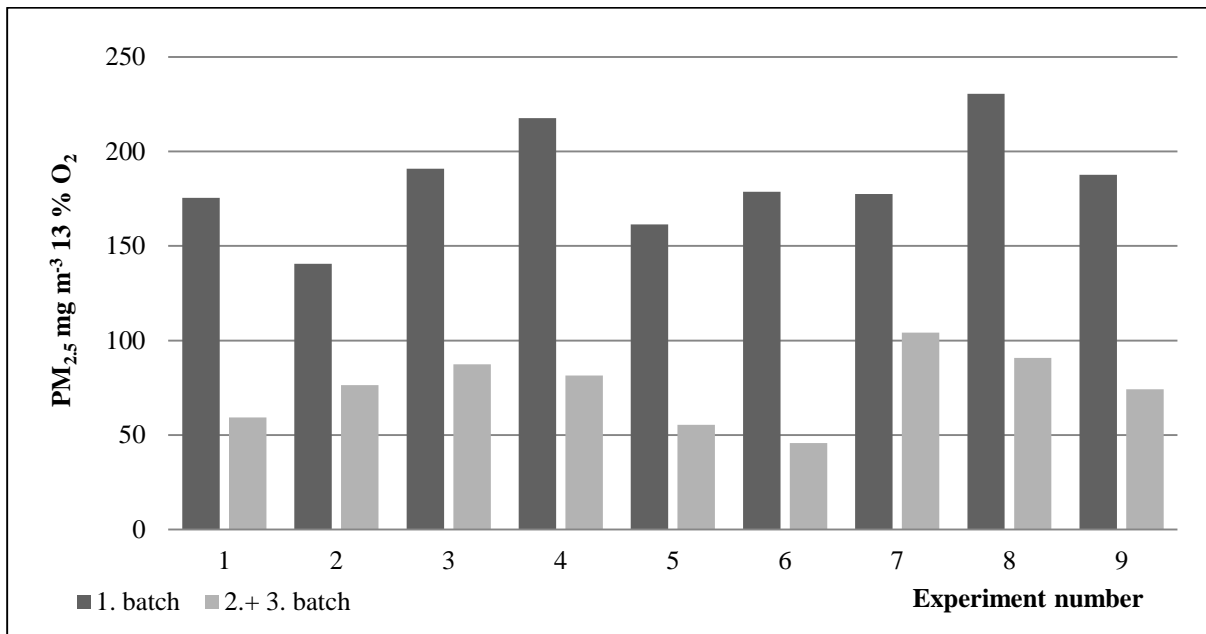
Figure 12. $PM_{2.5}$ concentration during the first batch (variation 141-231 mg m^{-3}) and during the second and the third batch (variation 46-104 mg m^{-3}) as measured with reference sampling filter collection.
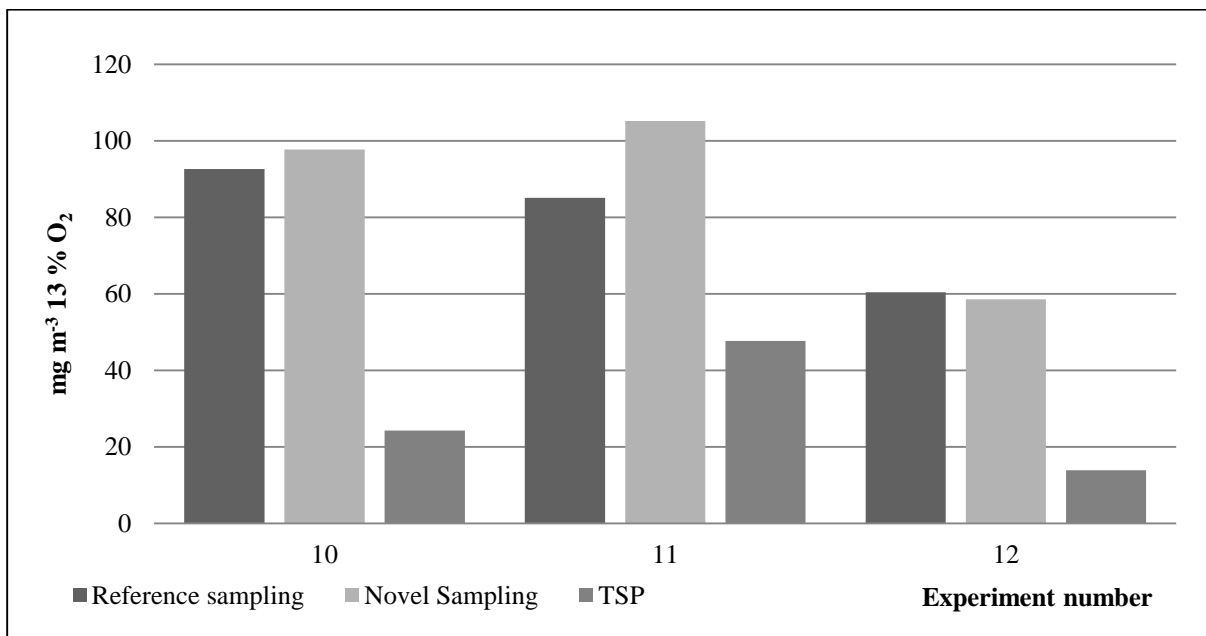
Figure 13. $PM_{2.5}$ concentration of the second batch as measured with reference sampling filter collection (variation 60-93 mg m^{-3}), novel sampling filter collection (variation 59-105 mg m^{-3}) and total suspended particles as measured with TSP filter collection (variation 14-48 mg m^{-3}).

The sampling methods were compared in the experiments 10 to 15. The average $PM_{2.5}$ concentrations of the reference and the novel sampling (Figure 13) were close to each other during the second batch. The maximum difference (experiment 11) was 19 %. The DR in reference sampling varied from 38 to 48 and in novel sampling from 25 to 34 and this difference did not seem to have great effect on the particle mass concentration.

The share of coarse particles (particles larger than 2.5 µm) in the total particle mass during the second batch was 8.8 % and 7.9 % as measured with the novel sampling. In the reference sampling the share of $PM_{2.5-10}$ was 3.6 % in the second batch and 2.2 % in the whole combustion. The share of particles larger than 10 µm was 2.3 % in the second batch and 0.5 % in the whole combustion. It can be concluded that the particle mass concentrations were clearly dominated by the fine particles. One has to remember, though, that the sampling was not isokinetic which surely caused loss of the larger particles. These losses were not measured.

In every experiment the TSP method gave significantly lower concentrations than the reference sampling method and the novel sampling method as can be seen from Figures 13 and 14. On average, the results of reference sampling were 2.7-fold higher in the second batch and 3.5-fold higher in the whole combustion. This can mainly be attributed to the treatment of the quartz filter in the TSP method. Before and after the sample collection the filter is heated before weighing to ensure the complete vaporization of water from the filter. Besides water, the heating probably causes vaporization and loss of some HCs which lowers the mass of the sample. In addition, the TSP method is developed to measure particle concentrations from large scale power plants where the flue gas velocities are higher and flows are quite laminar. In small-scale combustion appliances the flue gas flow is slower and more turbulent.
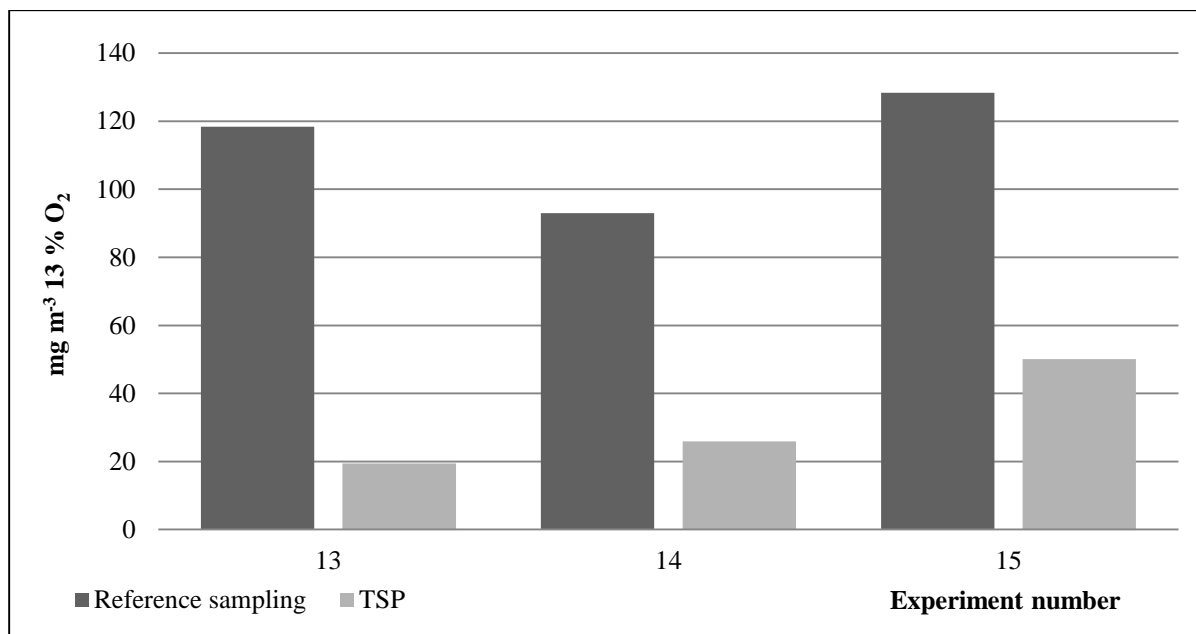
Figure 14. PM$_{2.5}$ concentration of the whole combustion (three batches) as measured with reference sampling filter collection (variation 93-128 mg m^{-3}) and total suspended particles as measured with TSP filter collection (variation 19-50 mg m^{-3}).

The reference sampling PM$_{2.5}$ concentration correlated well with the other indicators of incomplete combustion, OGC and CO, as the coefficients of determination (R^2) were 0.72 and 0.86, respectively.

The TEOM data processing is illustrated in Figure 15. The exceptionally high concentrations in the beginning (about 700-2000 mg m^{-3}) were removed from the 30 second average data. This was done because the high concentrations affected the average concentrations significantly and TEOM 30 second data was not comparable with the reference sampling filter collection. In 5 minute average data the same problem did not exist because the average was calculated over a longer time period where lower concentrations were already included. The same removal of exceptionally high concentrations was repeated with TEOM data in every experiment.
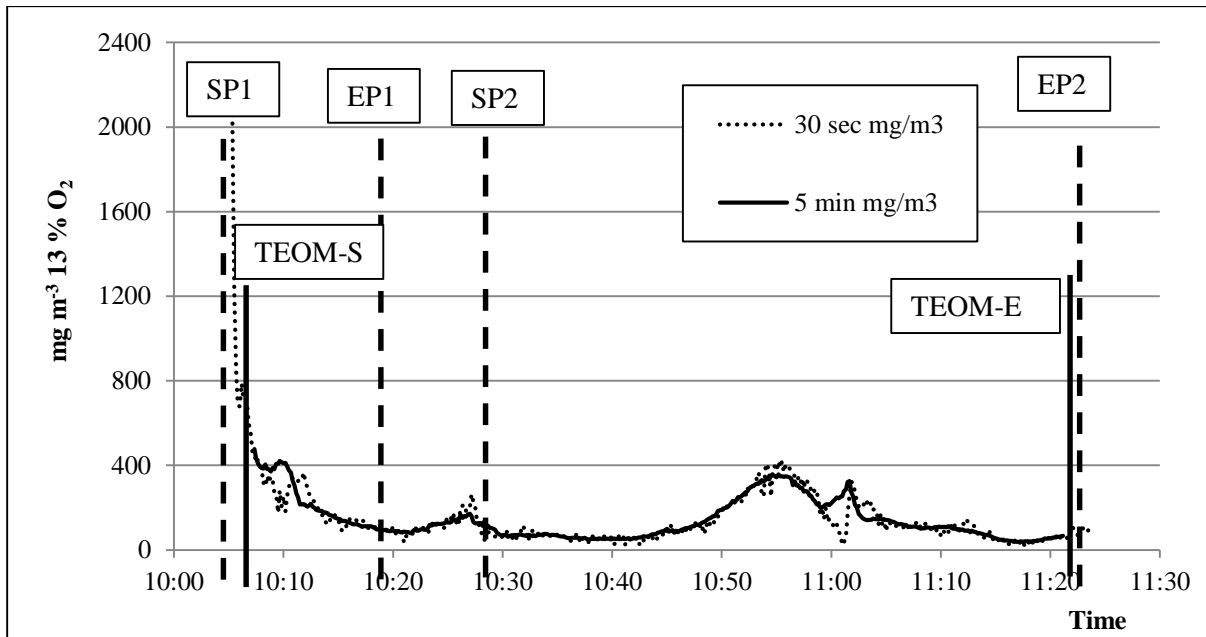
Figure 15. Illustration of TEOM data processing in experiment 8. Dashed vertical line is the start and the end point of the filter collection in reference sampling, solid vertical line is the start and the end point of calculation of the TEOM 30 sec particle mass average. SP1, start point of the first filter collection; EP1, end point of the first filter collection; SP2, start point of the second filter collection; EP2, end point of the second filter collection; TEOM-S, start point TEOM calculation; TEOM-E, end point of TEOM calculation.

Results of the TEOM PM mass concentration (the ones corresponding the filter collections) are presented in Figures 16 and 17. In all experiments 30 second and 5 minute averages gave almost equal concentrations. During the first batch 30 second average was 200 mg m^{-3} and 5 minute average was 208 mg m^{-3}. The time averages during the sampling of the second and the third batch were same, 102 mg m^{-3}. The average concentrations in the second batch (30 second 131 mg m^{-3}, 5 minute 128 mg m^{-3}), were close to the whole combustion averages (30 second 133 mg m^{-3}, 5 minute 130 mg m^{-3}). Concentrations measured with TEOM were slightly higher than the ones measured with the sampling which is logical since no pre-impactor was in use with TEOM. The difference was most evident in the concentrations of the second batch as TEOM concentration was 1.6-fold to reference sampling. The minimal differences between the results suggest that the measurements with TEOM were reliable and operating of the MMH was repeatable. In addition, TEOM 5 minute average particle mass correlated well with the PM$_{2.5}$ as measured with reference sampling filter collection (R^2 = 0.93). (Figure 18). Both methods seemed to be suitable for particle mass measurements.
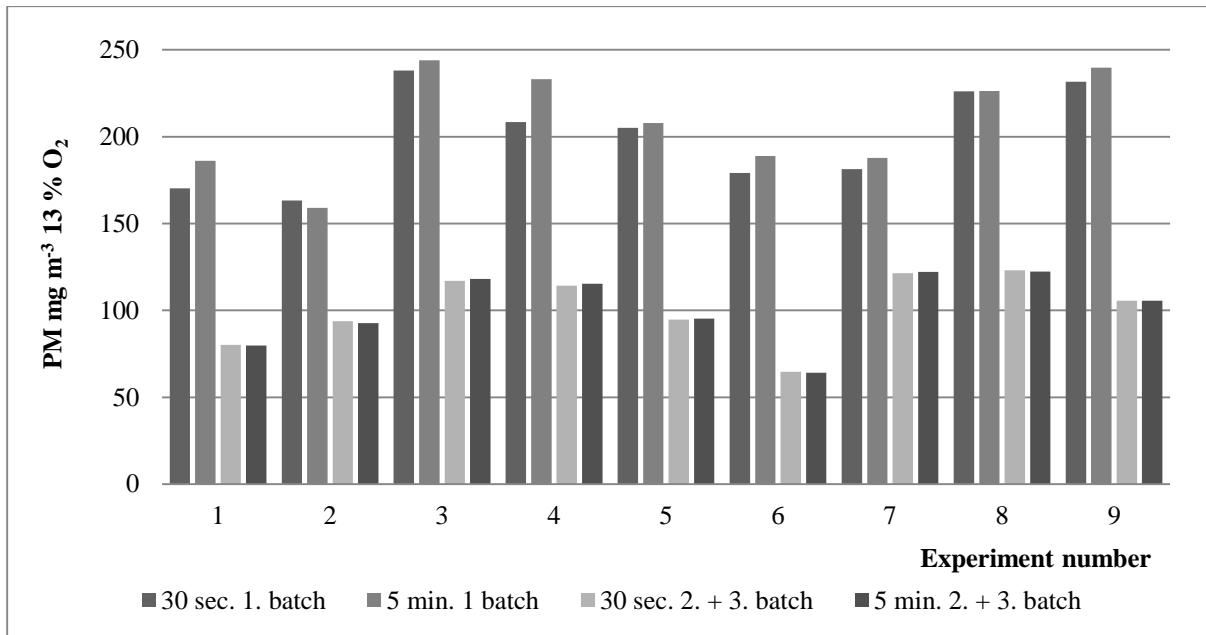
Figure 16. PM mass concentration during the first batch and during the second and the third batch presented as TEOM 30 seconds and 5 minute averages. Variations: 30 seconds 1. batch (163-238 mg m^{-3}), 5 minute 1. batch (159-244 mg m^{-3}), 30 seconds 2. + 3. batch (65-123 mg m^{-3}), 5 minute 2. + 3. batch (64-122 mg m^{-3}).
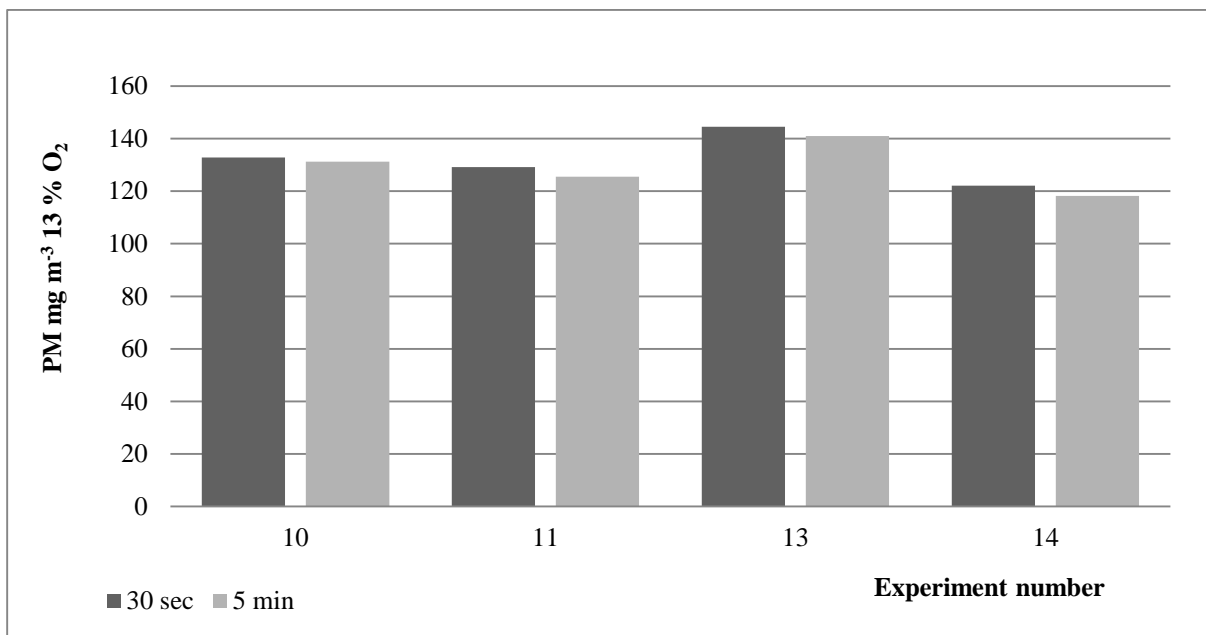
Figure 17. PM mass concentration of the second batch (experiments 10-11) and the whole combustion (experiments 13-14) presented as TEOM 30 seconds and 5 minute averages.
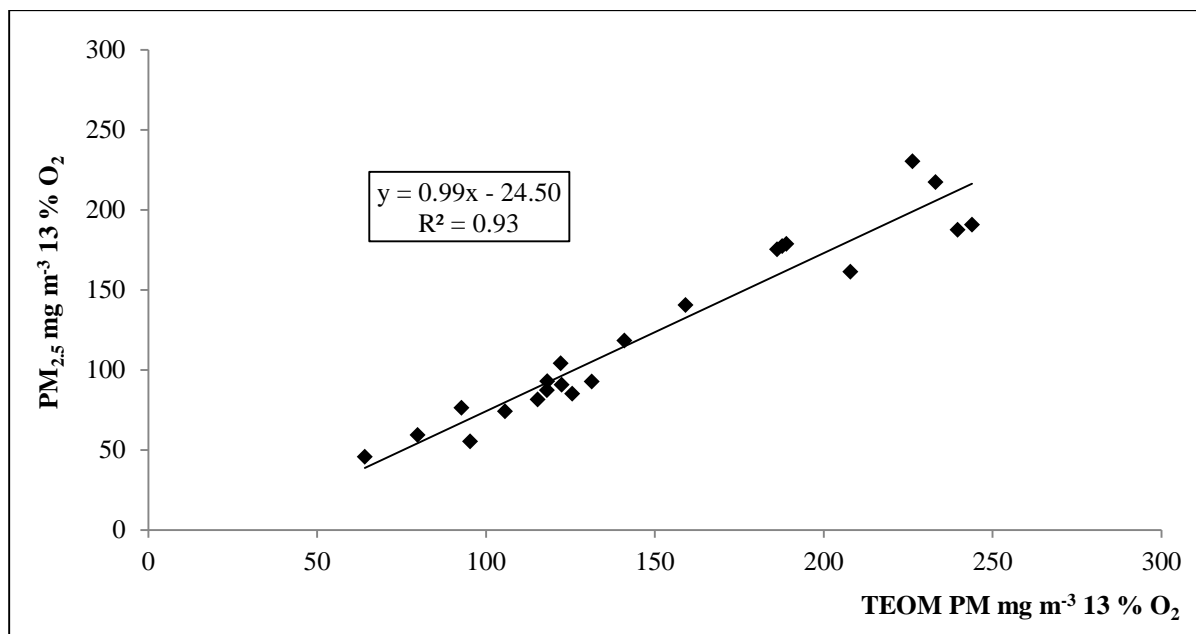
Figure 18. Reference sampling filter collection $PM_{2.5}$ concentration as a function of TEOM 5 min PM mass concentration.

The time series of the TEOM particle mass concentration, ELPI and CPC particle number concentrations and ELPI particle GMD from experiment 6 are presented in Figure 19. The CPC number concentrations were highest in the first batch (about 1.5-fold to second and third batch) but difference was not as great as it was in the particle mass concentrations (filter collections and TEOM) discussed earlier. In CPC clear peaks could be seen when a new batch was added. This was probably a result of accelerated pyrolysis caused by the hot furnace (Tissari, 2008a). ELPI number concentration was nearly stable during the whole combustion. The CPC average number concentration in the whole combustion varied from 2.9×10^7 to 4.6×10^7 # cm^{-3}. The particle GMD measured with ELPI remained quite stable through the combustion and the average in experiment 6 was 55 nm. TEOM 30 second and 5 minute averages are in line with each other. The whole combustion variations were 95-161 mg m^{-3} for 30 second and 97-159 mg m^{-3} for 5 minute averages.

ELPI particle number concentration was clearly higher than CPC number concentration, about 3.3-fold on average during the whole combustion. This might be due to an error which is caused by ELPI particle charging: larger particles are easily charged multiple times which results in too high particle number concentration. CPC, on the other hand, is considered to be reliable in particle number measurements. (Hämeri and Mäkelä, 2005.) This explanation could be too straightforward, though. Leskinen et al. (2012) investigated eight different measurement devices with synthetic test particles. They pointed out that differences between

the results of the devices might arise not only from different operation principles of the devices but also from different properties of the particles in question. Regardless of the different results between the devices the results were usually at an acceptable level.

The ELPI particle number size distributions from every experiment are collected to Figure 20. Distributions are unimodal and majority of the particles were in the ultrafine size fraction (dp < 100 nm).
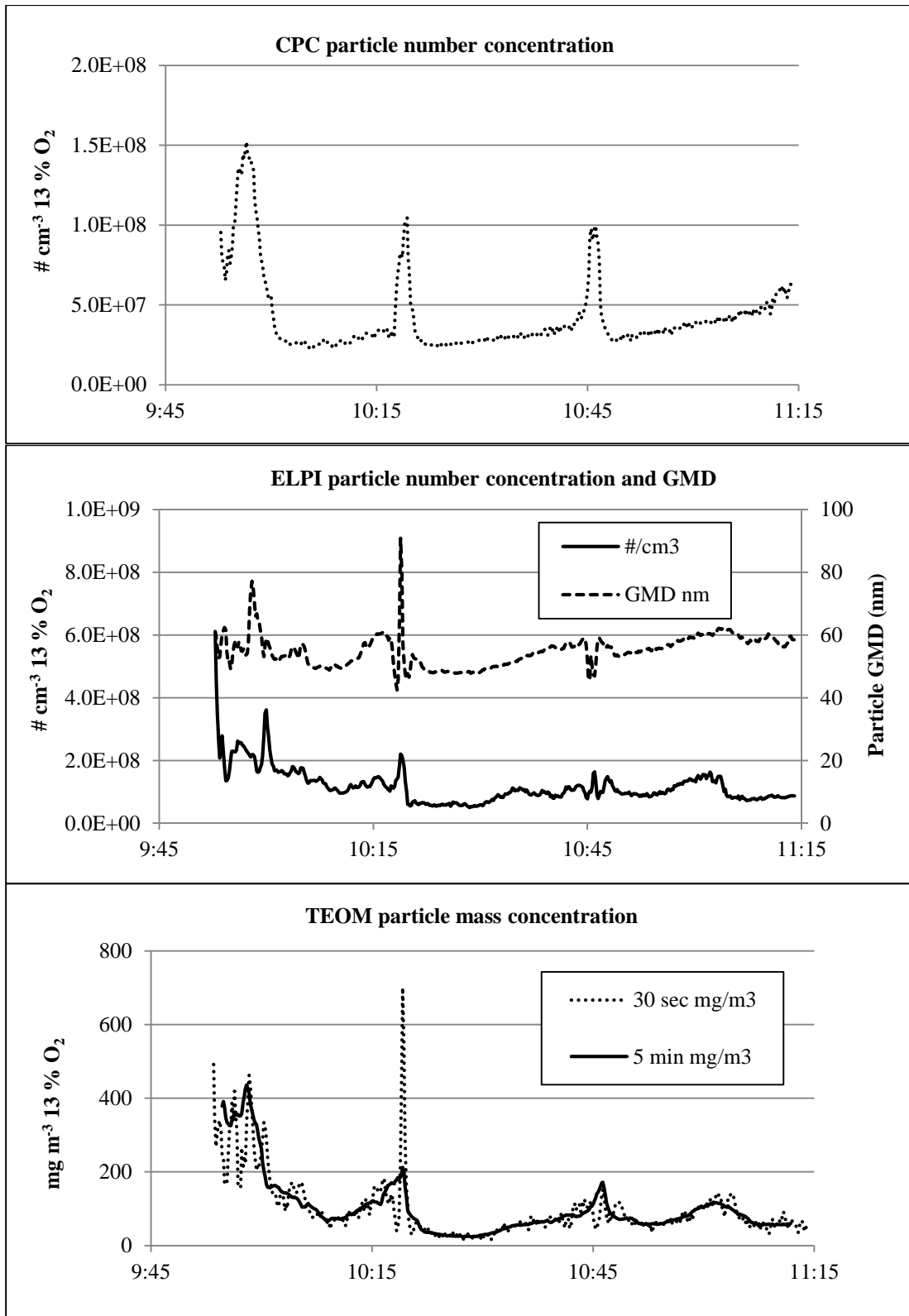
Figure 19. Experiment 6 time series of TEOM particle mass concentration, ELPI particle number concentration and geometric mean diameter and CPC particle number concentration.
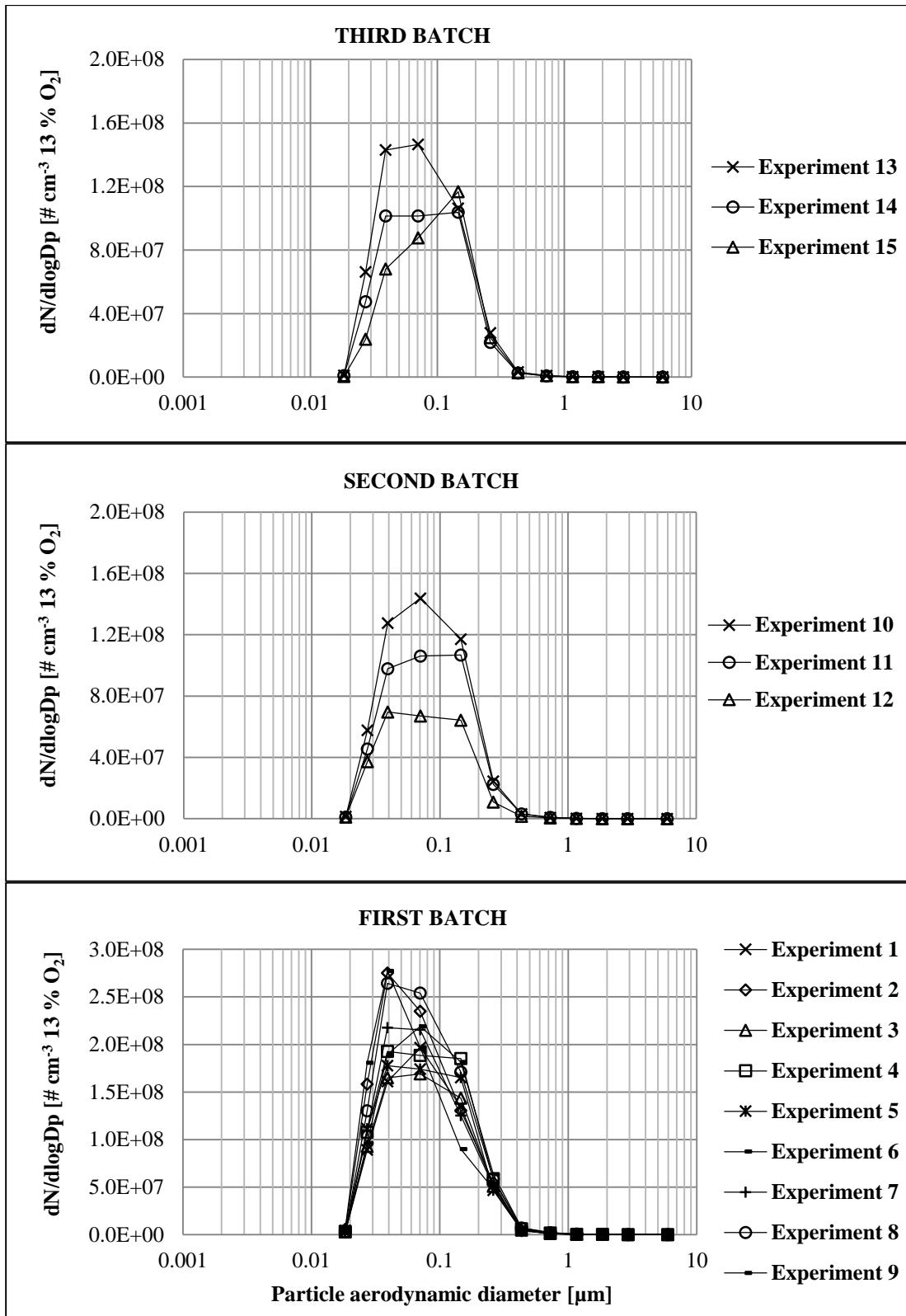
Figure 20. ELPI particle number size distributions of the first, the second and the third batch.

In Table 4 is a comparison of the particle emission factors between TS-MMH and MMH, conventional masonry heater (CMH) and sauna stove (SS) (Tissari et al., 2007; 2008a; 2008b) and continuous pellet burner (PB) (Lamberg et al., 2011).

The fine particle mass emissions from TS-MMH were 2-fold higher than the emissions from other studied MMHs (Tissari et al. 2007 and 2008a) and from CMH (Tissari et al. 2008a). Mass emissions from CMH studied by Tissari et al. (2008b) were slightly higher than TS-MMH. Emissions from sauna stove (SS) are known to be high. Particle mass emission was clearly higher in SS, about 3.5-fold to TS-MMH. The benefits of continuous pellet combustion are obvious when it comes to reducing emissions. The difference in particle number emissions was not that great between appliances and according to Tissari (2008) number emission alone is not a good indicator to estimate how complete the combustion is.

The greater GMD in Tissari et al. (2008a) could be explained with different collection plates applied in ELPI. Greased aluminium foils seemed to collect bigger particles than sintered collection plates. One reason to this could be particle bounce (Hinds, 1999) when particles do not attach to the collection plates in question but tend to bounce back to the sample stream. With greased aluminium foils the goal has been to diminish this phenomenon. According to Marjamäki and Keskinen (2004) increased roughness in collection plate leads to less steep collection efficiency curve and because of this, the impactor should be recalibrated if collection plates are changed.

Results of ELPI particle GMD have be interpreted with care, however. Leskinen et al. (2012) tested ELPI with three different collection plates: greased aluminium foils, sintered and bare steel. The differences in measured particle size with different collection plates increased as the complexity of the particle morphology increased via agglomeration. The conclusion was that the different results could mainly be attributed to nature of the test particles, not with applied collection plates.

Table 4. Comparison of the whole combustion average particle mass emission factors (filter collection), ELPI particle number emission factors and ELPI particle GMD between different studies and combustion appliances. In Tissari et al. (2007, 2008a and 2008b) and in Lamberg et al. (2011) the PM size is PM_1. MMH, modern masonry heater; CMH, conventional masonry heater; SS, sauna stove; PB, pellet boiler.

Emission parameter	This study	Tissari et al. (2008a)			Tissari et al. (2008b)	Tissari et al. (2007)		Lamberg et al. (2011)
	MMH	MMH	CMH	SS	CMH	MMH	CMH	PB
PM (mg MJ^{-1})	76	38	38	273	98	38	44	12.2
ELPI N (# MJ^{-1})	8.2E+13	3.2E+13	1.7E+13	9.8E+13	2.1E+14	4.4E+13	1.7E+14	1.6E+13
ELPI GMD (nm)	66[b]	130[a]	150[a]	110[a]	65[b]	83[b]	64[b]	69[b]
Fuel	Birch	Birch	Birch	Birch	Birch	Birch	Birch	Pine

[a] 9 out of 11 experiments had aluminum foils as collection plates.

[b] sintered collection plates in all experiments

5.3 PARTICLE CHEMICAL COMPOSITION

The results of the thermal-optical carbon analysis are presented in Figure 21. Fine particles consisted mainly of EC which comprised 62-94 % of the particle mass while the shares of OC were much lower (0-27 %). In Figure 21 the non-carbonaceous components are referred to as "Other". The negative shares of OC and other components in some experiments resulted from the uncertainty of the thermal-optical method.
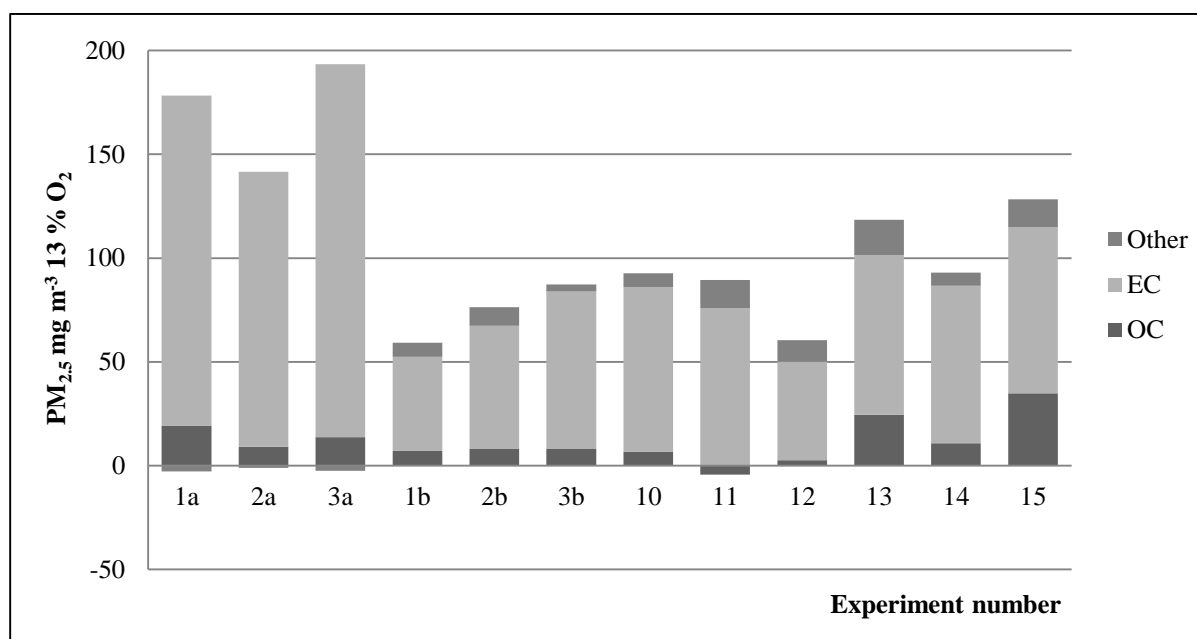
Figure 21. Organic carbon and elemental carbon of PM$_{2.5}$ in the first batch (experiments 1a-3a), in 2.+3. batch (experiments 1b-3b), in the second batch (experiments 10-12) and in the whole combustion (experiments 13-15) as measured with thermal-optical method.

In PM emissions from TS-MMH the share of EC was much higher compared to previous studies. Tissari et al. (2007 and 2008b) measured EC shares of 30 % and 32 %, respectively. The results of Frey et al. (2009) were similar to these as the share of EC was 32 %. In Schmidl et al. (2008) the portions of EC varied between wood species but were still lower than in this study; 19-31 %.

High share of EC means that the combustion conditions were poor in some way. One reason might have been that the TS-MMH had a quite small furnace (width 0.295 m, depth 0.4 m). Probably because of this the residence time of soot particles in the combustion zone was not long enough. In addition, during the combustion the flame was often in contact with the furnace window or the back wall of the furnace. This caused deposition of the particles on the

furnace surfaces which was quite visible. The contact with the window may have caused the flame temperature to drop which, together with possibly short residence time, resulted in insufficient combustion of the soot particles. The secondary air feed from the top of the furnace could have cooled the flame even further. Apart from this, the deposited soot particles may have later been ejected into the flue gas without going through proper combustion.

5.4 COMPARISON WITH DIRECTIVE 2009/125/EC

Specific requirements for emissions from local space heaters are presented in a draft prepared by European Commission (2013). The draft concerns the implementation of the energy efficiency -directive (2009/125/EC) and the new appliances have to meet the requirements by 1st of January 2018.

The emission limits are given in concentration averages. For the gaseous emissions the proposed limits are: 80 mg m^{-3} for OGC, 1500 mg m^{-3} for CO, 200 mg m^{-3} for NO$_x$. The PM emission limits depend on the applied sampling method. For TSP (or "PM measurement by sampling a partial flue gas sample over a heated filter") the limit is 40 mg m^{-3} and for diluted sample (filter at ambient temperature) the limit is 73.6 mg m^{-3}. All of the gaseous emissions from TS-MMH fulfill the emission requirements as the concentrations were 31 mg m^{-3} (OGC), 142 mg m^{-3} (NO$_x$), and 444 mg m^{-3} (CO). PM concentration measured using TSP method (32 mg m^{-3}) was below the limit but the concentration in the diluted sample (113 mg m^{-3} as measured with the reference sampling method) exceeded the limit. The TEOM average whole combustion PM concentrations exceeded the limit as well as the results were 127 mg m^{-3} (TEOM 30 sec) and 127 mg m^{-3} (TEOM 5 min).

5.5 USABILITY OF THE NOVEL SAMPLING METHOD

Altogether, the novel sampling method required quite a lot of monitoring. The importance of critical orifices remained a little vague because dilution had to be continuously monitored by following the CO$_2$ concentrations and if necessary, adjusted with the needle valve. The ball valve in the end of the sampling line used for adjusting the sample stream was very responsive – already a small adjustment had a big effect on the sample flow. Replacing it with a less-responsive valve would make the adjustment easier.

The DR of the novel sampling increased towards the end of the combustion. This was due to increased temperature which increased the sample volume and diluted it even further. Increase in the DR was more evident in the reference sampling. The difference might result simply from continuous monitoring and adjustment of the novel sampling DR. Yet, unexplainable oscillations of the DR occurred from time to time (Figure 24). In Figure 24 the reference sampling was in use from the beginning of the combustion but the novel sampling was used only to measure the second batch (start time 10:22). This is why DR is exceptionally high when the sampling begins. It could be possible to stabilize the DR by stabilizing the flue gas temperature by heating the sampling line before the diluters.

The filter collection itself was pretty easy to execute. PARAFILM® was needed to seal the $PM_{2.5}$ separator and also some parts of the sampling line which was not a problem. The assembling of the sampling line itself could be reconsidered. Replacing some of the rigid metal parts with elastic hoses could make the sampling line easier to transport from one measuring site to another. Of course the filter holder -part needs to be robust but assembling the whole sampling line rigidly made the whole system little unstable.
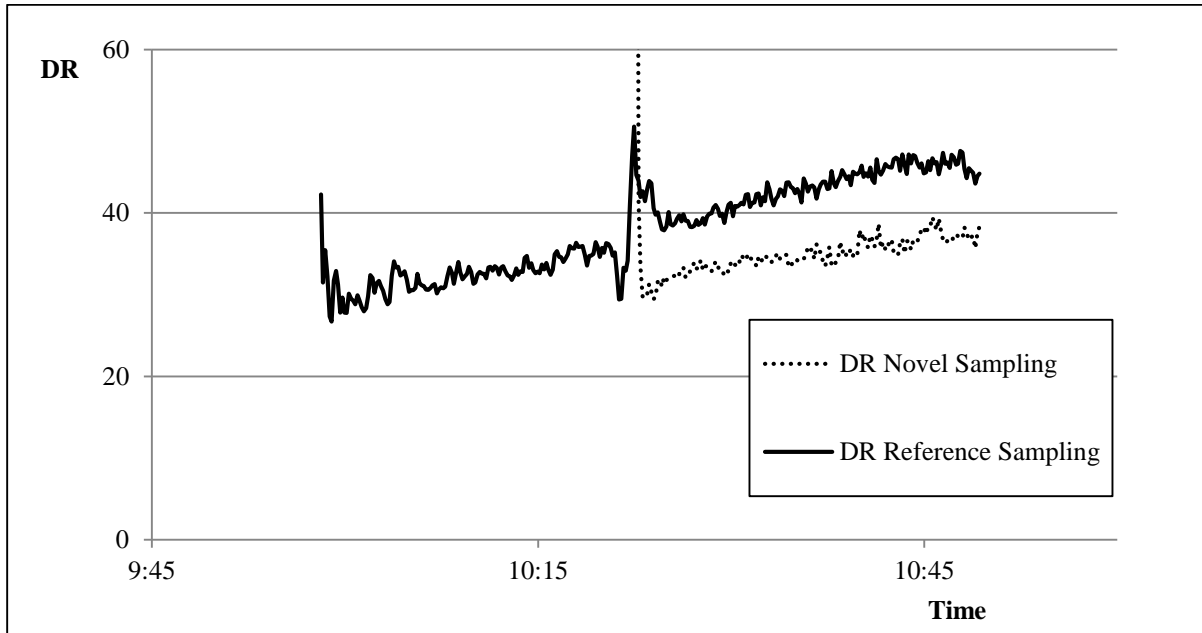

Figure 24. Dilution ratios of reference sampling and novel sampling in experiment 11.

6. CONCLUSIONS

In this study particle and gaseous emissions were measured from batch-wise operated modern masonry heater. Measurements were done with different continuous devices and filter collections. Obtained results were compared between the applied methods and legislation.

Clearly the highest mass emissions of particulate matter (PM), carbon monoxide (CO) and gaseous hydrocarbons (HCs) formed during the first batch. The main reason to this was probably the cold furnace which lowered the burnout temperature. When a new batch was added the emissions increased temporarily due to accelerated pyrolysis caused by the hot furnace. Vast majority of the particle mass emission consisted of particles smaller than 2.5 μm in aerodynamic diameter ($PM_{2.5}$). Small changes in the dilution ratio did not seem to affect the $PM_{2.5}$ concentration. Particle number emissions were also highest during the first batch and majority of the particles were ultrafine (smaller than 100 nm in aerodynamic diameter).

The curiosity was that the share of elemental carbon (EC) in $PM_{2.5}$ was very high when compared to other studied appliances in the literature. The reason to this was probably a decrease in the flame temperature due to its contact to the hatch window. Also, the secondary air feed probably lowered the flame temperature even further.

The best qualities of the studied appliance were low emissions of CO and gaseous HCs. Emissions of nitrogen oxides (NO_x) were similar to other studies and maintained quite stable throughout the combustion. Masonry heater fulfills the requirements of the upcoming EU emission requirements in the gaseous emissions and in the PM emissions measured from the hot flue gas. The PM concentrations measured from the diluted sample exceeded the limits.

The tested novel sampling system required quite a lot of monitoring and adjustment as the goal was to maintain the dilution ratio steady. The filter collection of the novel sampling was fluent to execute but the transportability of the sampling system could be improved by replacing some of the metal parts with elastic hoses.

REFERENCES

Asumisen rahoitus- ja kehittämiskeskus (ARA), The Housing Finance and Development Centre of Finland. (2013). *Energia-avustusohje 2013.*

Cape Grim Greenhouse Gas Data. (2013). Available at http://www.csiro.au/greenhouse-gases/. Accessed 4th December 2013.

Dekati Ltd. (2008). *ELPI^{TM} User Manual.*

Directive 2009/28/EC of the European parliament and of the council of 23 April 2009 on the promotion of the use of energy from renewable sources and amending and subsequently repealing Directives 2001/77/EC and 2003/30/EC. Official Journal of the European Union. L 140/16.

Directive 2009/125/EC of the European parliament and of the council of 21 October 2009 establishing a framework for the setting of ecodesign requirements for energy-related products. Official Journal of the European Union. L 285/10.

European Commission. (2013). *Ecodesign legislation, a draft for implementing Directive 2009/125/EC of the European Parliament and of the Council with regard to ecodesign requirements for local space heaters.* Brussels, Belgium.

European Commission. (2005). *Commission Staff working paper SEC (2005) 1133. Annex to the Communication on Thematic Strategy on Air Pollution and The Directive on "Ambient Air Quality and Cleaner Air for Europe.* Brussels, Belgium.

Fine Particle and Aerosol Technology Laboratory (FINE). PUPO-database, Puun pienpolton päästö- ja toksisuustietokanta. University of Eastern Finland. Available at http://wanda.uef.fi/pupo/info.html. Accessed 2nd of September 2013.

Flagan, R. C. and Seinfeld, J. H. (1988). *Fundamentals of air pollution engineering.* Prentice-Hall Inc., New Jersey.

Forster, P., Ramaswamy, V., Artaxo, P., Berntsen, T., Betts, R., Fahey, D.W., Haywood, J., Lean, J., Lowe, D.C., Myhre, G., Nganga, J., Prinn, R., Raga, G., Schulz, M. and Van Dorland, R. (2007). *Changes in Atmospheric Constituents and in Radiative Forcing.* In: Solomon, S., Qin, D., Manning, M., Chen, Z., Marquis, M., Averyt, K.B., Tignor, M. and Miller, H. L. (eds.) *Climate Change 2007: The Physical Science Basis. Contribution of Working Group I to the Fourth Assessment Report of the Intergovernmental Panel on Climate Change.* Cambridge University Press, Cambridge, United Kingdom and New York, NY, USA.

Frey, A.K., Tissari, J., Saarnio, K.M., Timonen, H.J., Tolonen-Kivimäki, O., Aurela, M.A, Saarikoski, S.K., Makkonen, U., Hytönen, K., Jokiniemi, J., Salonen, R.O. & Hillamo, R.E.J. (2009). *Chemical composition and mass size distribution of fine particulate matter emitted by a small masonry heater.* Boreal Environment Research, 14, 255-271.

Glasius, M., Ketzel, M., Wåhlin, P., Jensen, B., Mønster, J., Berkowicz, R., Palmgren, F. (2006). *Impact of wood combustion on particle levels in a residential area in Denmark.* Atmospheric Environment, 40, 7115-7124.

Hellén, H., Hakola, H., Haaparanta, S., Pietarila, H., Kauhaniemi, M. (2008). *Influence of residential wood combustion on local air quality.* Science of The Total Environment, 393, 283-290.

Hedberg, E., Kristensson, A., Ohlsson, M., Johansson, C., Johansson, P-Å., Swietlicki, E., Vesely, V., Wideqvist, U., Westerholm, R. (2002). *Chemical and physical characterization of emissions from birch wood combustion in a wood stove.* Atmospheric Environment, 36, 4823-4837.

Hinds, W. C. (1999). *Aerosol Technology: Properties, Behaviour, and Measurement of Airborne Particles.* 2nd edition. John Wiley & Sons, Inc. New York.

Huotari, J. and Vesterinen, R. (2002). *Muut polton päästöt.* In: Raiko, R., Saastamoinen, J., Hupa, M., Kurki-Suonio, I. (eds.) *Poltto ja palaminen.* 2nd edition. Teknistieteelliset akatemiat, Helsinki.

Hytönen, K., Jokiniemi, J., Obernberger, I., Brunner, T., Salonen, R. O., Aurela, M., Bellmann, B., Boman, C., Bärnthaler, G., Ellner-Schubert, F., Forsberg, B., Frey, A., Friesenbicher, J., Happo, M., Hartmann, H., Hillamo, R., Hirvonen, M-R., Jalava, P., Markkanen, P., Pennanen, A., Pettersson, E., Roßmann, P., Saarikoski, S., Saarnio, K., Sandström, T., Sehlstedt, M., Sillanpää, M., Teinilä, K., Timonen, H., Tissari, J., Turowski, P., Vallius, M., Wiinikka, H. (2008). *Biomass combustion in residential heating: particulate measurements, sampling, and physicochemical and toxicological characterization.* Report series of Department of Environmental Science, University of Kuopio.

Hämeri, K. and Mäkelä, J. (2005). *Differentiaalinen liikkuvuusanalysaattori (DMA).* In: Hämeri, K. and Mäkelä, J. *Aerosolien mittaustekniikka.* University of Helsinki.

Iisa, K., Yrjas, P., Kilpinen. P. (2002). *Rikin oksidien muodostuminen ja poistaminen.* In: Raiko, R., Saastamoinen, J., Hupa, M., Kurki-Suonio, I. (eds.) *Poltto ja palaminen.* 2nd edition. Teknistieteelliset akatemiat, Helsinki.

Jokiniemi, J. and Kauppinen, E. (2002). *Polttoprosessien aerosolit.* In: Raiko, R., Saastamoinen, J., Hupa, M., Kurki-Suonio, I. (eds.) *Poltto ja palaminen.* 2nd edition. Teknistieteelliset akatemiat, Helsinki.

Jucks, K. W., Johnson, D. G., Chance, K. V., Traub, W. A. (1996). *Ozone production and loss rate measurements in the middle stratosphere.* Journal of Geophysical Research, 101, 28,785-28,792.

Karppinen, A., Härkönen, J., Kukkonen, J., Aarnio, P., Koskentalo, T. (2004). *Statistical model for assessing the portion of fine particulate matter transported regionally and long range to urban air.* Scandinavian Journal of Work, Environment & Health, 30, 47-53.

Karvosenoja, N., Tainio, M., Kupiainen, K., Tuomisto, J. T., Kukkonen, J., Johansson, M. (2008). *Evalutation of the emissions and uncertainties of PM2.5 originated from vehicular traffic and domestic wood combustion in Finland.* Boreal Environment Research, 13, 465 – 474.

Karvosenoja, N., Kupiainen, K., Paunu, V-V., Savolahti, M. (2012). *Pienpolton hiukkasten ja mustahiilen päästöt sekä niille altistuminen.* Finnish Environment Institute (SYKE). Available at http://www.hsy.fi/seututieto/Documents/ilmanlaatu_tutkimusseminaari/tutkimusseminaari2012/Karvosenoja_HSY2012.pdf. Accessed 29th of August 2013.

Kilpinen, P. (2002a). *Palamisen kemiaa.* In: Raiko, R., Saastamoinen, J., Hupa, M., Kurki-Suonio, I. (eds.) *Poltto ja palaminen.* 2nd edition. Teknistieteelliset akatemiat, Helsinki.

Kilpinen, P. (2002b). *Typen oksidien muodostuminen ja hajoaminen.* In: Raiko, R., Saastamoinen, J., Hupa, M., Kurki-Suonio, I. (eds.) *Poltto ja palaminen.* 2nd edition. Teknistieteelliset akatemiat, Helsinki.

Knudsen, J.N., Jensen, P.A., Dam-Johansen, K. (2004). *Transformation and Release to the Gas Phase of Cl, K, and S during Combustion of Annual Biomass.* Energy & Fuels, 18, 1385-1399.

Lamberg, H., Sippula, O., Tissari, J., Jokiniemi, J. (2011). *Effects of Air Staging and Load on Fine-Particle and Gaseous Emissions from a Small-Scale Pellet Boiler.* Energy & Fuels, 25, 4952-4960.

Leskinen, J., Joutsensaari, J., Lyyränen, J., Koivisto, J., Ruusunen, J., Järvelä, M., Tuomi, T., Hämeri, K., Auvinen, A., Jokiniemi, J. (2012). *Comparison of nanoparticle measurement instruments for occupational health applications.* Journal of Nanoparticle Research, 14, 1-16.

Lipsky, E. M. & Robinson, A. L. (2006). *Effects of Dilution on Fine Particle Mass and Partitioning of Semivolatile Organics in Diesel Exhaust and Wood Smoke.* Environmental Science & Technology, 40, 155 – 162.

Marjamäki, M. and Keskinen, J. (2004). *Effect of impaction plate roughness and porosity on collection efficiency.* Journal of Aerosol Science, 35, 301-308.

NIOSH (National Institute for Occupational Safety and Health). (1999). *Elemental carbon (diesel particulate): Method 5040.* NIOSH Manual of Analytical Methods (NMAM), Fourth Edition.

Patashnick, H., Meyer, M., Rogers, B. (2002). *Tapered element oscillating microbalance technology.* Proceedings of the North American/Ninth U.S. Mine Ventilation Symposium, 625-631.

Pope, C. A. & Dockery, D. W. (2006). *Health Effects of Fine Particulate Air Pollution: Lines that Connect.* Air & Waste Management Association, 56, 709-742.

Ramanathan, V. & Carmichael, G. (2008). *Global and regional climate changes due to black carbon.* Nature Geoscience, 1, 221-227.

Saastamoinen, J. (2002). *Kiinteän polttoaineen palaminen ja kaasutus*. In: Raiko, R., Saastamoinen, J., Hupa, M., Kurki-Suonio, I. (eds.) *Poltto ja palaminen*. 2nd edition. Teknistieteelliset akatemiat, Helsinki.

Salonen, R. O. and Pennanen A. (2007). *The Impact of Fine Particles on Health. Views and Conclusions from the FINE Particles – Technology, Environment and Health Technology Programme*. Tekes, Helsinki.

Schmidl, C., Marr, I. L., Caseiro, A., Kotianová, P., Berner, A., Bauer, H., Kasper-Giebl, A., Puxbaum, H. (2008). *Chemical characterisation of fine particle emissions from wood stove combustion of common woods growing in mid-European Alpine regions*. Atmospheric Environment, 42, 126-141.

Sims, R.E.H., Schock, R. N., Adegbululgbe, A., Fenhann, J., Konstantinaviciute, I., Moomaw, W., Nimir, H.B., Schlamadinger, B., Torres-Martínez, J., Turner, C., Uchiyama, Y., Vuori, S.J.V., Wamukonya, N. and Zhang, X. (2007). *Energy supply*. In: Metz, B., Davidson, O.R., Bosch, P.R., Dave, R. and Meyer, L.A. (eds.) *Climate Change 2007: Mitigation. Contribution of Working Group III to the Fourth Assessment Report of the Intergovernmental Panel on Climate Change*. Cambridge University Press, Cambridge, United Kingdom and New York, NY, USA.

SFS, Finnish Standards Association. (1990). *SFS 5624: Air quality. Stationary source emissions. Determination of flue gas conditions*. Finnish Standards Association, Helsinki.

Szidat, S., A. S. H. Prévôt, J. Sandradewi, M. R. Alfarra, H.-A. Synal, L. Wacker, U. Baltensperger. (2007). *Dominant impact of residential wood burning on particulate matter in Alpine valleys during winter*. Geophysical Research Letters, 34.

Statistics Finland, Energy (2012). *Energy consumption in households 2011*. Helsinki, Finland.

Statistics Finland, Energy (2013). *Energy prices 2013, 1st quarter*. Helsinki, Finland.

Thermo Nicolet Corp. (2001). *Introduction to Fourier Transform Infrared Spectrometry*.

Thermo Scientific[TM]. *TEOM Series 1405 Ambient Particulate Monitor*. Product Specifications.

Tissari, J. (2008). *Fine Particle Emissions from Residential Wood Combustion*. Department of Environmental Science, University of Kuopio. Doctoral thesis.

Tissari J., Hytönen, K., Lyyränen, J., Jokiniemi, J. (2007). *A novel field measurement method for determining fine particle and gas emissions from residential wood combustion*. Atmospheric Environment, 41, 8330 – 8344.

Tissari, J., Hytönen, K., Sippula, O., Jokiniemi, J. (2008a). *The effects of operating conditions on emissions from masonry heaters and sauna stoves*. Biomass and Bioenergy, 33, 513-520.

Tissari, J., Lyyränen, J., Hytönen, K., Sippula, O., Tapper, U., Frey, A., Saarnio, K., Pennanen, A. S., Hillamo, R., Salonen, R. O., Hirvonen, M.-R., Jokiniemi, J. (2008b). *Fine particle and gaseous emissions from normal and smouldering wood combustion in a conventional masonry heater.* Atmospheric Environment, 42, 7862-7873.

TSI Inc. (2012). *Condensation Particle Counter Model 3775*.

Valtion Teknillinen Tutkimuskeskus VTT, Technical Research Centre of Finland. (2000). *Suomessa käytettävien polttoaineiden ominaisuuksia*. Espoo, Finland.

Volkamer, R., Jimenez, J. L., San Martini, F., Dzepina, K., Zhang, Q., Salcedo, D., Molina, L. T., Worsnop, D. R., Molina, M. J. (2006). *Secondary organic aerosol formation from anthropogenic air pollution: Rapid and higher than expected.* Geophysical Research Letters, 33.

World Health Organization (WHO). (2006). *WHO Air Quality Guidelines, Global Update 2005. Particulate matter, ozone, nitrogen dioxide and sulfur dioxide.* WHO Regional Office for Europe, Copenhagen, Denmark.

Zachowski, E. J. and Paleologos, S. (2009). *Flame Ionization Detectors: Applications and Operations.* Specialty Gas Report, Second Quarter.

Tables of gaseous emissions

Table 1. Concentrations (average ± standard deviation) of CO_2 and O_2 in volume percentages and concentrations of OGC, CO and NO_x per combustion phase in mg m^{-3} normalized into 13 % O_2.

Combustion phase	CO$_2$ %	O$_2$ %	OGC	CO	NO$_x$
1. batch	7.5 ± 1.2	13.5 ± 1.2	97 ± 53	1070 ± 265	181 ± 81
2. + 3. batch	8.5 ± 0.6	12.3 ± 0.6	5.3 ± 1.3	184 ± 35	85 ± 29
2. batch	7.2 ± 0.5	13.8 ± 0.6	4.9 ± 1.3	271 ± 56	167 ± 77
3. batch	8.2 ± 0.3	12.6 ± 0.4	3.1 ± 0.91	174 ± 80	227 ± 46
Whole combustion	8.1 ± 0.7	12.8 ± 0.7	31 ± 13	444 ± 102	142 ± 78

Table 2. Emission factors (average ± standard deviation) of OGC, CO and NO_x per combustion phase in mg MJ^{-1}.

Combustion phase	OGC	CO	NO$_x$
1. batch	66 ± 36	580 ± 144	79 ± 21
2. + 3. batch	3.5 ± 0.89	99 ± 19	52 ± 8.7
2. batch	3.3 ± 0.85	146 ± 31	56 ± 12
3. batch	2.1 ± 0.61	94 ± 43	57 ± 12
Whole combustion	21 ± 8.6	240 ± 55	61 ± 10.4

Table 3. Emission factors (average ± standard deviation) of gaseous hydrocarbons per combustion phase in mg MJ^{-1}.

Combustion phase	CH$_4$	Acetylene	Benzene	Toluene
1. batch	18 ± 7.3	5.7 ± 2.7	3.3 ± 1.4	3.5 ± 0.79
2. + 3. batch	1.8 ± 0.25	0.84 ± 0.17	0.088 ± 0.061	2.04 ± 0.31
2. batch	1.9 ± 0.35	1.06 ± 0.25	0.25 ± 0.13	2.9 ± 0.77
3. batch	1.6 ± 0.49	0.88 ± 0.12	0.089 ± 0.047	2.4 ± 0.708
Whole combustion	6.5 ± 2.04	2.3 ± 0.67	1.03 ± 0.49	2.6 ± 0.65

Table 4. Emission factors (average ± standard deviation) of gaseous hydrocarbons per combustion phase in mg MJ^{-1}.

Combustion phase	Formic acid	Acetic acid	Formalde-hyde	Acetalde-hyde	Methanol
1. batch	2.4 ± 1.1	28 ± 17	15 ± 7.3	5.2 ± 3.5	17 ± 12
2. + 3. batch	0.57 ± 0.26	0.69 ± 0.29	0.46 ± 0.16	0.109 ± 0.084	0.039 ± 0.035
2. batch	0.69 ± 0.33	0.59 ± 0.39	0.53 ± 0.28	0.11 ± 0.12	0.041 ± 0.049
3. batch	0.38 ± 0.44	0.54 ± 0.39	0.36 ± 0.203	0.13 ± 0.12	0.056 ± 0.063
Whole combustion	1.1 ± 0.39	9.1 ± 5.4	4.8 ± 2.3	1.7 ± 1.07	5.5 ± 3.6

Table 5. Concentrations (average ± standard deviation) of gaseous hydrocarbons per combustion phase in mg m^{-3} normalized into 13 % O_2.

Combustion phase	CH$_4$	Acetylene	Benzene	Toluene
1. batch	29 ± 13	10.4 ± 4.9	8.5 ± 6.7	10.1 ± 7.9
2. + 3. batch	2.8 ± 0.603	1.3 ± 0.39	0.15 ± 0.064	3.8 ± 1.4
2. batch	2.8 ± 0.82	1.9 ± 0.44	0.77 ± 0.39	12 ± 8.6
3. batch	1.7 ± 0.52	1.5 ± 0.205	0.46 ± 0.24	15 ± 4.3
Whole combustion	9.5 ± 3.09	3.8 ± 1.03	2.8 ± 2.6	8.4 ± 7.4

Table 6. Concentrations (average ± standard deviation) of gaseous hydrocarbons per combustion phase in mg m^{-3} normalized into 13 % O_2.

Combustion phase	Formic acid	Acetic acid	Formalde-hyde	Acetalde-hyde	Methanol
1. batch	4.5 ± 2.1	67 ± 53	27 ± 14	11 ± 8.3	33 ± 23
2. + 3. batch	0.94 ± 0.55	1.1 ± 0.47	0.704 ± 0.19	0.19 ± 0.18	0.055 ± 0.047
2. batch	1.3 ± 0.64	1.9 ± 1.6	1.03 ± 0.57	0.26 ± 0.29	0.085 ± 0.104
3. batch	0.75 ± 0.87	2.1 ± 1.5	0.72 ± 0.405	0.38 ± 0.34	0.12 ± 0.13
Whole combustion	1.9 ± 0.78	22 ± 19	8.4 ± 4.4	3.6 ± 2.7	9.8 ± 6.9

Tables of particle emissions

Table 1. Particle mass concentrations normalized into 13 % O_2 (average ± standard deviation) measured with TEOM and filter collections. RS, reference sampling; NS, novel sampling.

Combustion phase	TEOM mg m^{-3}		RS PM$_{2.5}$	NS PM$_{2.5}$	TSP
	30 sec	5 min	mg m^{-3}	mg m^{-3}	mg m^{-3}
1. batch	190 ± 27	190 ± 33	184 ± 27		
2. + 3. batch	105 ± 23	105 ± 23	75 ± 19		
2. batch	130 ± 11	127 ± 12	79 ± 17	87 ± 25	29 ± 17
3. batch	119 ± 11	119 ± 11			
Whole combustion	127 ± 21	127 ± 20	113 ± 18		32 ± 16

Table 2. Particle mass emission factors (average ± standard deviation) measured with TEOM and filter collections. RS, reference sampling; NS, novel sampling.

Combustion phase	TEOM mg MJ^{-1}		RS PM$_{2.5}$	NS PM$_{2.5}$	TSP
	30 sec	5 min	mg MJ^{-1}	mg MJ^{-1}	mg MJ^{-1}
1. batch	128 ± 19	129 ± 22	126 ± 19		
2. + 3. batch	71 ± 15	71 ± 15	51 ± 13		
2. batch	87 ± 8	86 ± 9	53 ± 11	59 ± 17	19 ± 12
3. batch	80 ± 8	80 ± 8			
Whole combustion	86 ± 14	86 ± 14	76 ± 12		21 ± 11

Table 3. Particle GMD (average ± standard deviation) per combustion phase as measured with ELPI, particle number concentrations and particle number emission factors as measured with ELPI and CPC per combustion phase. p (%) = precision percentage (= standard deviation / average × 100) .

Combustion phase	GMD nm	ELPI # cm^{-3}	p. (%)	ELPI # MJ^{-1}	p. (%)	CPC # cm^{-3}	p. (%)	CPC # MJ^{-1}	p. (%)
1. batch	66 ± 5	1.7E+8	15	1.1E+14	16	3.9E+7	20	2.6E+13	20
2. + 3. batch	64 ± 4	1.1E+8	12	7.1E+13	12	3.7E+7	16	2.5E+13	16
2. batch	69 ± 5	1.1E+8	24	7.2E+13	25	3.0E+7	10	2.0E+13	10
3. batch	75 ± 10	1.0E+8	18	6.9E+13	18	3.0E+7	3	2.0E+13	3
Whole combustion	66 ± 5	1.2E+8	10	8.2E+13	11	3.7E+7	13	2.5E+13	13